



HAL
open science

A methods assessment and recommendations for improving calculations and reducing uncertainties in the determination of ^{210}Po and ^{210}Pb activities in seawater

Sylvain Rigaud, V. Puigcorbé, P. Cámara-Mor, N. Casacuberta, M. Roca-Martí, J. Garcia-Orellana, C. Benitez-Nelson, P. Masque, T. Church

► To cite this version:

Sylvain Rigaud, V. Puigcorbé, P. Cámara-Mor, N. Casacuberta, M. Roca-Martí, et al.. A methods assessment and recommendations for improving calculations and reducing uncertainties in the determination of ^{210}Po and ^{210}Pb activities in seawater. *Limnology and Oceanography: Methods*, 2013, 11 (10), pp.561-571. 10.4319/lom.2013.11.561 . hal-01717794

HAL Id: hal-01717794

<https://hal.science/hal-01717794>

Submitted on 27 Feb 2018

HAL is a multi-disciplinary open access archive for the deposit and dissemination of scientific research documents, whether they are published or not. The documents may come from teaching and research institutions in France or abroad, or from public or private research centers.

L'archive ouverte pluridisciplinaire **HAL**, est destinée au dépôt et à la diffusion de documents scientifiques de niveau recherche, publiés ou non, émanant des établissements d'enseignement et de recherche français ou étrangers, des laboratoires publics ou privés.

1 **A methods assessment and recommendations for improving calculations and reducing uncertainties**
2 **in the determination of ^{210}Po and ^{210}Pb activities in seawater**

3
4 Rigaud¹, S., Puigcorb ^{2,3}, V., C mara-Mor^{2,3}, P., Casacuberta^{2,3}, N., Roca-Mart ^{2,3}, M., Garcia-Orellana^{2,3},
5 J., Benitez-Nelson⁴, C.R., Masqu ^{2,3}, P., and Church^{1*}, T.

6
7 ¹School of Marine Science and Policy, University of Delaware, Newark, Delaware 19716 USA.

8 ²Departament de F sica, Universitat Aut noma de Barcelona, Barcelona 08193 Spain.

9 ³Institut de Ci ncia i Tecnologia Ambientals, Universitat Aut noma de Barcelona, Barcelona 08193 Spain.

10 ⁴Marine Science Program and Department of Earth and Ocean Sciences, University of South Carolina,
11 South Carolina 29208 USA.

12

13

14 **Running Head:** ^{210}Po and ^{210}Pb activity calculations in seawater

15

16

17

18

*Corresponding author

tchurch@udel.edu

Phone: (302) 831-2558

Fax: (302) 831-4575

19 **Acknowledgements**

20 The National Science Foundation grants (OCE-0851462) contributed to the manuscript and (OCE -
21 0961653) provided support for S. Rigaud. V. Puigcorbé, P. Cámara-Mor and M. Roca-Martí acknowledge
22 funding through PhD grants from the Ministerio de Educación y Ciencia (Spain). Funding was also
23 obtained through the ICREA Academia prize of the Generalitat de Catalunya and MEC CTM2007-31241-
24 E/MAR (P. Masque) and EU FP7-MC-IIF-220485 (C.R. Benitez-Nelson and P. Masqué). S. Rigaud also
25 wishes to thank Rachel Shelley for her initial assistance in writing the paper.

26

27

28 **Abstract**

29 In marine systems, ^{210}Po and ^{210}Pb disequilibria are being increasingly used to examine oceanic
30 particle formation and export. Here, an updated assessment of current methods for determining ^{210}Po and
31 ^{210}Pb activity in marine samples is provided and includes a complete description of the vast number of
32 calculations and uncertainties associated with Po and Pb loss, decay, and ingrowth during sample
33 processing. First we summarize the current methods for the determination of ^{210}Po and ^{210}Pb activities in
34 dissolved and particulate seawater samples and recommend areas for improvement. Next, we detail the
35 calculations and associated uncertainties using principles of error propagation, while also accounting for
36 radionuclide ingrowth, decay and recovery. A spread-sheet reporting these calculations is included as a
37 downloadable Web Appendix. Our analysis provides insight into the contributions of the relative
38 uncertainty for each parameter considered in the calculation of final ^{210}Po and ^{210}Pb activities and gives
39 recommendations on how to obtain the most precise final values. For typical experimental conditions in
40 open seawater, we show that our method allows calculating ^{210}Pb activity with a relative uncertainty of
41 about 7%. However for ^{210}Po activities, the final relative uncertainty is more variable and depends on the
42 $^{210}\text{Po}/^{210}\text{Pb}$ activity ratio in the initial sample and the time elapsed between sampling and sample
43 processing. The lowest relative uncertainties on ^{210}Po that can be obtained by this method is 6% and can
44 only be obtained for samples with high $^{210}\text{Po}/^{210}\text{Pb}$ activity ratios (>1) that were rapidly processed.

45

46

47 **Introduction**

48 The naturally occurring ^{210}Po ($T_{1/2} = 138.4$ d) and ^{210}Pb ($T_{1/2} = 22.3$ y) radionuclide pair has been
49 widely used to examine dissolved and particle dynamics in marine eco-systems over the past several
50 decades (Bacon *et al.* 1976; Nozaki *et al.* 1976; Thomson and Turekian 1976; Masqué *et al.* 2002; Cochran
51 and Masqué 2003; Rutgers van der Loeff and Geibert 2007). Both nuclides are part of the ^{238}U decay
52 chain, with ^{210}Po produced from the decay of ^{210}Pb via ^{210}Bi ($T_{1/2} = 5.0$ d). In seawater, both ^{210}Pb and
53 ^{210}Po are particle reactive, but ^{210}Po also bio-accumulates within organic tissues (Stewart and Fisher
54 2003a, 2003b; Stewart *et al.* 2005). As such, differences in the specific activity of these two radionuclides
55 in the water column have been increasingly used to quantitatively assess export fluxes of sinking
56 particulate material, such as organic carbon, from the surface ocean to depth (Moore and Dymond 1988;
57 Sarin *et al.* 1999; Friedrich and Rutgers van der Loeff 2002; Stewart *et al.* 2007; Verdeny *et al.* 2009;
58 Yang *et al.* 2011).

59 Since the fundamental measurement techniques described by Fler and Bacon (1984), there have
60 been significant improvements in sample processing that rely on the use of exchange resins (Sarin *et al.*
61 1992, Vajda *et al.*, 1994). While these methods have proven to be very successful in the separation of Po
62 and Pb, losses of ^{210}Pb can occur during processing. Unfortunately, there is no clear consensus as to how
63 such losses should be assessed during subsequent calculations. Some laboratories consider the loss as
64 minor and ignore it, while others include extensive correction procedures. In addition, each laboratory has
65 their own approach for calculating radionuclide ingrowth, decay and recovery during sample processing as
66 well as error treatment, which relies on a range of assumptions. As a result, questions have been raised
67 regarding the accuracy and precision of ^{210}Po and ^{210}Pb measurements in seawater (Church, *et al.*, 2012).

68 An initial assessment of the precision and accuracy of current procedures for ^{210}Po and ^{210}Pb
69 measurement was conducted as part of a recent intercalibration exercise using dissolved and particulate
70 seawater samples (Church *et al.* 2012). One of the major conclusions was that, while the results reported
71 by laboratories agree relatively well (relative standard deviation, $\text{RSD} < 50\%$) for samples with high ^{210}Po

72 and ^{210}Pb activities (>0.1 dpm), this agreement became rather poor (RSD up to 200%) for lower activity
73 samples. Although the authors were not able to precisely identify the sources of the disagreements, they
74 suggested that one possibility includes the manner in which the ^{210}Po and ^{210}Pb ingrowth, decay and
75 recovery calculations were conducted. Their study further revealed that there were various methodologies
76 in how uncertainties and error propagation were considered, which resulted in a large range in the specific
77 activity uncertainties reported. The inter-calibration effort by [Church et al. \(2012\)](#), therefore suggests that
78 there is a need for the scientific community to concur on “best practices” for ^{210}Po and ^{210}Pb measurement
79 as well as final data calculations.

80 In this context, the aims of this paper are: (1) to review the protocols used for ^{210}Po and ^{210}Pb
81 measurements in seawater and provide recommendations for improving the method’s accuracy, (2) to
82 detail the calculations necessary for including isotopic recoveries and decay/ingrowth corrections during
83 sample processing, (3) to develop a protocol for error propagation and to identify the main sources of
84 uncertainty in the final data, and (4) to recommend methods for lowering the relative uncertainty. A
85 practical spread-sheet, which follows step wise the complex formulations reported in the paper, has been
86 made available as an downloadable Web Appendix.

87

88 **Materials and Procedures**

89 *General procedure for sample collection and processing*

90 A typical protocol used for seawater sample processing of ^{210}Pb and ^{210}Po is presented in Figure 1
91 and assumes analysis of ^{210}Po and ^{210}Pb by alpha spectrometry as described by [Fleer and Bacon \(1984\)](#).
92 The seawater sample is collected as either total (unfiltered) or dissolved (filtered) with the particulate
93 fraction measured separately. After collection, the dissolved or total sample is acidified to pH 1-2 with
94 HCl, spiked with a well-calibrated ^{209}Po tracer solution ($T_{1/2}=102$ y) and a well-standardized stable lead
95 carrier added in order to monitor the losses of Po and Pb during sample processing. Some laboratories also
96 use ^{208}Po ($T_{1/2} = 2.9$ y) in a double spike technique, the former added to monitor the initial yield and the
97 latter to act as a second yield tracer ([Friedrich and Rutgers van der Loeff 2002](#)). In the following, we limit

98 our discussions to the single-²⁰⁹Po spike method, as tailing/peak overlap corrections for ²⁰⁸Po (alpha
99 energy of 5.11 MeV) and ²¹⁰Po (5.31 MeV) add another level of complexity not necessary for this
100 discussion (Fleer and Bacon 1984).

101 For both total and dissolved samples, Po and Pb can be pre-concentrated from large volumes of
102 seawater via co-precipitation with Fe(OH)₃ (Thomson and Turekian 1976; Nozaki 1986), Co-APDC (Fleer
103 and Bacon 1984) or MnO₂ (Bojanowski et al. 1983). The precipitate is then dissolved in an acid solution
104 (generally HCl for Fe(OH)₃ and MnO₂, HNO₃ for Co-APDC) and, after evaporation to near-dryness,
105 recovered in a 0.5-2M HCl solution. For particulate samples, the solid phase is completely dissolved using
106 a mixture of strong acids (including HF) and, after evaporation to near-dryness, also recovered in 0.5-2 M
107 HCl solution. The Po nuclides are then plated by spontaneous deposition onto a silver disc (Flynn 1968).
108 Silver discs, typically 1-2 cm in diameter, can be obtained with greater than 99.99% purity. They are first
109 shined with a commercial silver polish and then washed using water and ethanol. One side of the disc is
110 covered by an inert substance, such as rubber cement, electronic spray (e.g glyptol) or plastic tape, so that
111 Po nuclides are plated on only one side. For samples processed using Fe(OH)₃ co-precipitation, ascorbic
112 acid should be added to the plating solution before plating in order to avoid Fe(OH)₃ formation on the
113 plate. The Po activities are measured after deposition by alpha spectrometry. Any remaining ²¹⁰Po and
114 ²⁰⁹Po in solution is removed by either a second deposition onto another silver disc or scrap silver and/or
115 using anion exchange resin such as AG-1X8 (Sarin et al. 1992) or Sr Spec resin (Vajda, et al. 1994). Note
116 that the Po and Pb separation using Sr Spec resin can also be conducted prior to the first plating
117 (Bojanowski et al. 1983). After separation, the final eluate containing the ²¹⁰Pb is re-spiked with ²⁰⁹Po and
118 stored for greater than 6 months to allow in-growth of ²¹⁰Po from ²¹⁰Pb. At that time, the ²¹⁰Pb activity of
119 the sample is determined by replating the eluate solution on a new silver disc and measuring the in-growth
120 of ²¹⁰Po (Figure 1). The determination of the initial activities of ²¹⁰Po and ²¹⁰Pb in the sample at the time of
121 collection requires several corrections that account for decay and ingrowth between the time of collection
122 and processing, together with corrections for Po and Pb chemical recoveries (detailed in Section 3).

123

124 ***Improved accuracy of the method***

125 *Use of ion exchange resin for Po and Pb separation*

126 Complete removal of Po isotopes after the initial plating procedure is a key component for
127 increasing the accuracy of the method. Indeed, incomplete removal of Po isotopes prior to storage will
128 affect the final calculated ^{210}Pb activity, and thus that of ^{210}Po . There are two methods to remove the
129 residual Po isotopes: replating the solution or separation onto ion exchange resin. Replating of samples
130 may not be sufficient to ensure complete removal of residual Po as a fraction of the Po nuclides may
131 remain in solution. Based on the Po recovery efficiency obtained on about 80 processed samples, we
132 found that $17 \pm 19\%$ of the Po introduced into the plating solution can remain in solution after the first
133 plating. Note that such results are in agreement with previous findings (Flynn 1968). Assuming the same
134 efficiency for the cleaning plate, residual Po nuclides of $3 \pm 3\%$ will remain in solution. In contrast, ion
135 exchange experiments with spiked solutions of known amounts of ^{209}Po and ^{210}Po showed a quantitative
136 removal of Po ($98.9 \pm 1.4\%$, $n=6$, for AG-1X8 in HCl 9M; Rigaud unpublished results). Thus, although
137 both methods are valid, we recommend the use of ion exchange resin in order to obtain the most accurate
138 results.

139

140 *Precise determination of ^{210}Pb recovery efficiency during sample processing*

141 The Pb recovery is quantified by measuring stable lead concentrations in known aliquots of the
142 plating solution. Usually only one aliquot is collected after the second plating, providing information on
143 the total Pb loss that occurs during complete sample processing. This loss is generally assumed to occur
144 only during sample extraction (filtered or unfiltered) or dissolution (particulate). For example experiments
145 using the most common extraction protocols ($\text{Fe}(\text{OH})_3$ and Co-APDC methods) on about 80 dissolved
146 seawater samples showed that the Pb extraction efficiency during initial seawater extraction were $70 \pm$
147 10% and $88 \pm 18\%$ for $\text{Fe}(\text{OH})_3$ and Co-APDC respectively. However, Pb losses have also been shown to
148 occur during ion exchange resin procedure. For comparison, the Pb recovery during resin separation was
149 $90 \pm 17\%$ and $96 \pm 16\%$ for the $\text{Fe}(\text{OH})_3$ and Co-APDC method respectively. Thus, although the Pb

150 recovery during the separation onto resin is significantly higher than during the extraction procedure, it is
151 not always complete and can constitute a non-negligible loss of Pb during sample processing. In the case
152 of particulate samples, for which no extraction is required (Figure 1), ion exchange separation is the main
153 step for Pb loss during sample processing. Thus precise assessment of Pb isotope loss during both
154 extraction and ion exchange procedure needs to be considered to accurately correct for the actual ^{210}Pb
155 fraction that leads to ^{210}Po ingrowth between the extraction and the first plating dates as well as during the
156 storage period. Therefore we strongly recommend collecting another aliquot of plating solution between
157 the first plating and the resin procedure (Figure 1). Note also that the fraction of the solution removed with
158 the aliquot, although small, must also be accounted for during the activity correction process. Indeed, the
159 fraction of ^{210}Pb removed with the aliquot will not contribute to ^{210}Po ingrowth during the storage period,
160 resulting in an underestimation of ^{210}Pb and an overestimation of ^{210}Po (Cf. Section 3).

161

162 **Assessment**

163 *Calculations and Associated Uncertainties*

164 In this section, calculations that correct for ^{210}Po and ^{210}Pb decay, ingrowth, and recovery are
165 presented along with their associated assumptions. The calculations are divided into several steps that
166 focus either on the activity of ^{210}Pb at the time of sample collection (Steps A) or ^{210}Po at the time of
167 sample collection (Steps B). The steps are presented in Figure 2 and consider three reservoirs: (1) the
168 sample (2) the plating solution in which Po and Pb are recovered after seawater extraction or particulate
169 dissolution, and (3) the two silver discs (the first one for the plating of *in situ* ^{210}Po and the second one for
170 the plating of ^{210}Po produced from the decay of ^{210}Pb during the storage period). A glossary of the terms
171 used is presented in Table 1. We also include equations that account for the combined uncertainty
172 calculated according to uncorrelated error propagation theory. The main sources of uncertainty we
173 consider here are those associated with (1) the counting of ^{210}Po and ^{209}Po by alpha spectrometry, (2) the
174 activity of the ^{209}Po spike, (3) the detector background, and (4) the Pb recovery. The uncertainties
175 associated with the radioactive decay constants of ^{210}Po , ^{210}Pb and ^{209}Po are ignored. The uncertainties

176 associated with the masses of sample, the spike and carrier amounts added into the sample, the mass of the
177 plating solution and the mass of aliquots taken for stable Pb analysis, are assumed to be of secondary
178 importance, and thus also ignored. However, if the additions of the ^{209}Po spike and Pb carrier are made
179 volumetrically, the volume used should be adapted to minimize uncertainties and the pipette should be
180 repeatedly calibrated for mass using the same solution and for each analyst. An analysis of the influence of
181 each of the uncertainties described above on the final ^{210}Po and ^{210}Pb calculated uncertainty, as well as
182 recommendations for minimizing some of these possible sources of error, are presented in Section 4.

183 An Excel spread-sheet including all calculations is available as a downloadable Web Appendix. In
184 these calculations the main assumptions are:

185 - (1) ^{210}Po and ^{209}Po are in chemical equilibrium at the time of co-precipitation and plating and are
186 scavenged and plated with the same efficiency. Such isotopic equilibrium is expected to be reached after
187 several hours of equilibration.

188 - (2) ^{210}Po activity on the silver discs decays only as a function of its own decay constant (i.e.,
189 ^{210}Pb is not plated onto the silver disc),

190 - (3) both ^{210}Po and ^{209}Po are completely removed from the plating solution after the first plating,
191 preferably using ion exchange resin or other quantitative procedure.

192 - (4) ^{210}Bi is at secular equilibrium with ^{210}Pb in the sample and plating solution, and thus, the in-
193 growth of ^{210}Po is only function of the ^{210}Pb decay.

194 - (5) ^{210}Pb activity in the sample and plating solutions decrease with time as a function of its own
195 decay constant (i.e. ^{210}Pb ingrowth from ^{226}Ra is assumed to be negligible during sample processing).

196

197 *Step A: Calculation of ^{210}Pb activity and associated uncertainty in the sample*

198 Step A-1: Calculation of ^{210}Po activity in the plating solution at the second plating date ($(A_{210\text{Po}})_{\text{sol,tplat2}}$),

199 dpm, Eq. 1a) and its associated uncertainty ($\sigma((A_{210\text{Po}})_{\text{sol,tplat2}})$, dpm, Eq. 1b) accounting for correction of

200 the detector background, Po recovery and ^{210}Po decay during counting and between the dates of second
 201 plating and second counting:

$$202 \quad (A_{210\text{Po}})_{\text{sol},t_{\text{plat}2}} = \left(\frac{C_{210\text{Po},2}}{T_{c2}} - (A_{210\text{Po}})_{\text{bg},2} \right) \frac{\lambda_{210\text{Po}} T_{c2}}{1 - e^{-\lambda_{210\text{Po}} T_{c2}}} \frac{(A_{209\text{Po}})_{\text{sp},t_{\text{cal}}} e^{-\lambda_{209\text{Po}}(t_{c2, \text{st}} - t_{\text{sp}, \text{cal}})} m_{\text{sp}2}}{\left(\frac{C_{209\text{Po},2}}{T_{c2}} - (A_{209\text{Po}})_{\text{bg},2} \right) \frac{\lambda_{209\text{Po}} T_{c2}}{1 - e^{-\lambda_{209\text{Po}} T_{c2}}}} e^{\lambda_{210\text{Po}}(t_{c2, \text{st}} - t_{\text{plat}2})}$$

203 *Eq. 1a*

$$204 \quad \sigma \left((A_{210\text{Po}})_{\text{sol},t_{\text{plat}2}} \right) =$$

$$205 \quad \sqrt{\begin{aligned} & \sigma(C_{210\text{Po},2})^2 \left(\frac{\lambda_{210\text{Po}}}{1 - e^{-\lambda_{210\text{Po}} T_{c2}}} \frac{(A_{209\text{Po}})_{\text{sp},t_{\text{cal}}} e^{-\lambda_{209\text{Po}}(t_{c2, \text{st}} - t_{\text{sp}, \text{cal}})} m_{\text{sp}2}}{\left(\frac{C_{209\text{Po},2}}{T_{c2}} - (A_{209\text{Po}})_{\text{bg},2} \right) \frac{\lambda_{209\text{Po}} T_{c2}}{1 - e^{-\lambda_{209\text{Po}} T_{c2}}}} e^{\lambda_{210\text{Po}}(t_{c2, \text{st}} - t_{\text{plat}2})} \right)^2 \\ & + \sigma((A_{210\text{Po}})_{\text{bg},2})^2 \left(\frac{\lambda_{210\text{Po}} T_{c2}}{1 - e^{-\lambda_{210\text{Po}} T_{c2}}} \frac{(A_{209\text{Po}})_{\text{sp},t_{\text{cal}}} e^{-\lambda_{209\text{Po}}(t_{c2, \text{st}} - t_{\text{sp}, \text{cal}})} m_{\text{sp}2}}{\left(\frac{C_{209\text{Po},2}}{T_{c2}} - (A_{209\text{Po}})_{\text{bg},2} \right) \frac{\lambda_{209\text{Po}} T_{c2}}{1 - e^{-\lambda_{209\text{Po}} T_{c2}}}} e^{\lambda_{210\text{Po}}(t_{c2, \text{st}} - t_{\text{plat}2})} \right)^2 \\ & + \sigma((A_{209\text{Po}})_{\text{sp},t_{\text{cal}}})^2 \left(\left(\frac{C_{210\text{Po},2}}{T_{c2}} - (A_{210\text{Po}})_{\text{bg},2} \right) \frac{\lambda_{210\text{Po}} T_{c2}}{1 - e^{-\lambda_{210\text{Po}} T_{c2}}} \frac{e^{-\lambda_{209\text{Po}}(t_{c2, \text{st}} - t_{\text{sp}, \text{cal}})} m_{\text{sp}2}}{\left(\frac{C_{209\text{Po},2}}{T_{c2}} - (A_{209\text{Po}})_{\text{bg},2} \right) \frac{\lambda_{209\text{Po}} T_{c2}}{1 - e^{-\lambda_{209\text{Po}} T_{c2}}}} e^{\lambda_{210\text{Po}}(t_{c2, \text{st}} - t_{\text{plat}2})} \right)^2 \\ & + \sigma(C_{209\text{Po},2})^2 \left(\left(\frac{C_{210\text{Po},2}}{T_{c2}} - (A_{210\text{Po}})_{\text{bg},2} \right) \frac{\lambda_{210\text{Po}} T_{c2}}{1 - e^{-\lambda_{210\text{Po}} T_{c2}}} \frac{(A_{209\text{Po}})_{\text{sp},t_{\text{cal}}} e^{-\lambda_{209\text{Po}}(t_{c2, \text{st}} - t_{\text{sp}, \text{cal}})} m_{\text{sp}2}}{(C_{209\text{Po},2} - T_{c2} (A_{209\text{Po}})_{\text{bg},2})^2} \frac{\lambda_{209\text{Po}}}{1 - e^{-\lambda_{209\text{Po}} T_{c2}}} e^{\lambda_{210\text{Po}}(t_{c2, \text{st}} - t_{\text{plat}2})} \right)^2 \\ & + \sigma((A_{209\text{Po}})_{\text{bg},2})^2 \left(\left(\frac{C_{210\text{Po},2}}{T_{c2}} - (A_{210\text{Po}})_{\text{bg},2} \right) \frac{\lambda_{210\text{Po}} T_{c2}}{1 - e^{-\lambda_{210\text{Po}} T_{c2}}} \frac{(A_{209\text{Po}})_{\text{sp},t_{\text{cal}}} e^{-\lambda_{209\text{Po}}(t_{c2, \text{st}} - t_{\text{sp}, \text{cal}})} m_{\text{sp}2} T_{c2}}{(C_{209\text{Po},2} - T_{c2} (A_{209\text{Po}})_{\text{bg},2})^2} \frac{\lambda_{209\text{Po}}}{1 - e^{-\lambda_{209\text{Po}} T_{c2}}} e^{\lambda_{210\text{Po}}(t_{c2, \text{st}} - t_{\text{plat}2})} \right)^2 \end{aligned}}$$

206 *Eq. 1b*

207
 208 Note that the recovery of ^{209}Po ($f_{\text{Po}, \text{rec}2}$) during the extraction and plating steps can be used as a quality
 209 control check of sample processing. It is determined as:

$$210 \quad f_{\text{Po}, \text{rec}2} = \frac{\left(\frac{C_{209\text{Po},2}}{T_{c2}} - (A_{209\text{Po}})_{\text{bg}} \right) \frac{\lambda_{209\text{Po}} T_{c2}}{1 - e^{-\lambda_{209\text{Po}} T_{c2}}}}{\varepsilon (A_{209\text{Po}})_{\text{sp},t_{\text{cal}}} e^{-\lambda_{209\text{Po}}(t_{c2, \text{st}} - t_{\text{sp}, \text{cal}})} m_{\text{sp}2}} \quad \text{Eq. 2a}$$

211
 212 Step A-2: Calculation of ^{210}Pb activity in the plating solution at the ion exchange resin separation date
 213 $((A_{210\text{Pb}})_{\text{sol}, \text{tres}}$, dpm, Eq. 3a) and its associated uncertainty $(\sigma((A_{210\text{Pb}})_{\text{sol}, \text{tres}}$, dpm, Eq. 3b) after correction
 214 for ^{210}Po in-growth and decay between the dates of resin separation and second plating:

215
$$(A_{210Pb})_{sol,t_{res}} = \frac{(A_{210Po})_{sol,t_{plat2}} (\lambda_{210Po} - \lambda_{210Pb})}{\lambda_{210Po} (e^{-\lambda_{210Pb}(t_{plat2}-t_{res})} - e^{-\lambda_{210Po}(t_{plat2}-t_{res})})}$$
 Eq. 3a

216
$$\sigma((A_{210Pb})_{sol,t_{res}}) = \sqrt{\sigma((A_{210Po})_{sol,t_{plat2}})^2 \left(\frac{(\lambda_{210Po} - \lambda_{210Pb})}{\lambda_{210Po} (e^{-\lambda_{210Pb}(t_{plat2}-t_{res})} - e^{-\lambda_{210Po}(t_{plat2}-t_{res})})} \right)^2}$$
 Eq. 3b

217

218 Step A-3: Calculation of ^{210}Pb activity in the sample at sampling date $((A_{210Pb})_{spl,t_{spl}}$, dpm, Eq. 4a) and its

219 associated uncertainty $(\sigma((A_{210Pb})_{spl,t_{spl}})$, dpm, Eq. 4b) accounting for correction for ^{210}Pb decay between

220 the dates of resin separation and sampling, Pb recoveries and blank:

221
$$(A_{210Pb})_{spl,t_{spl}} = \frac{(A_{210Pb})_{sol,t_{res}} e^{\lambda_{210Pb}(t_{res}-t_{spl})}}{f_{Pbrec,tot}} \left(1 + \frac{m_{al1}}{m_{sol1}}\right) - (A_{210Pb})_B$$
 Eq. 4a

222
$$\sigma((A_{210Pb})_{spl,t_{spl}}) = \sqrt{\sigma((A_{210Pb})_{sol,t_{res}})^2 \left(\frac{e^{\lambda_{210Pb}(t_{res}-t_{spl})}}{f_{Pbrec,tot}} \left(1 + \frac{m_{al1}}{m_{sol1}}\right) \right)^2 + \sigma(f_{Pbrec,tot})^2 \left(\frac{(A_{210Pb})_{sol,t_{res}} e^{\lambda_{210Pb}(t_{res}-t_{spl})}}{(f_{Pbrec,tot})^2} \left(1 + \frac{m_{al1}}{m_{sol1}}\right) \right)^2 + \sigma((A_{210Pb})_B)^2}$$
 Eq. 4b

223

224 $f_{Pbrec,tot}$ and its associated uncertainty $\sigma(f_{Pbrec,tot})$ represents the total Pb recovery efficiency during the

225 sample processing, which includes Pb loss during the extraction from seawater samples or particulate

226 dissolution and during the ion exchange resin separation procedure. It is obtained by :

227
$$f_{Pbrec,tot} = \frac{m_{sol2}[Pb]_{sol2} + m_{al1}[Pb]_{sol1}}{m_c[Pb]_c}$$
 Eq. 5a

228
$$\sigma(f_{Pbrec,tot}) = \sqrt{\sigma([Pb]_{sol2})^2 \left(\frac{m_{sol2}}{m_c[Pb]_c} \right)^2 + \sigma([Pb]_{sol1})^2 \left(\frac{m_{al1}}{m_c[Pb]_c} \right)^2 + \sigma([Pb]_c)^2 \left(\frac{m_{sol2}[Pb]_{sol2} + m_{al1}[Pb]_{sol1}}{m_c[Pb]_c^2} \right)^2}$$
 Eq. 5b

229

230 The parameters $(A_{210Pb})_B$ and $\sigma((A_{210Pb})_B)$ correspond to the activity (in dpm) and associated uncertainties,
 231 respectively, of ^{210}Pb in the blank that may be due to contamination of reagents (e.g., lead carrier). The
 232 blank is obtained by processing a volume of ultrapure water in the same manner as a sample, according to
 233 the procedure outlined in Figure 1 and calculated following steps A1 and A2, and replacing the equations
 234 of step A3 by:

$$235 \quad (A_{210Pb})_B = \frac{(A_{210Pb})_{sol,t_{res}} e^{\lambda_{210Pb}(t_{res}-t_{car})}}{f_{Pb,rec,tot}} \left(1 + \frac{m_{al1}}{m_{sol1}}\right) \quad \text{Eq. 6a}$$

$$236 \quad \sigma((A_{210Pb})_B) = \sqrt{\sigma((A_{210Pb})_{sol,t_{res}})^2 \left(\frac{e^{\lambda_{210Pb}(t_{res}-t_{car})}}{f_{Pb,rec,tot}} \left(1 + \frac{m_{al1}}{m_{sol1}}\right)\right)^2 + \sigma(f_{Pb,rec,tot})^2 \left(\frac{(A_{210Pb})_{sol,t_{res}} e^{\lambda_{210Pb}(t_{res}-t_{car})}}{(f_{Pb,rec,tot})^2} \left(1 + \frac{m_{al1}}{m_{sol1}}\right)\right)^2} \quad \text{Eq. 6b}$$

237
 238 Step A-4: Final calculation of ^{210}Pb activity in the sample at the sampling date $((A_{210Pb})_{spl,t_{spl}})$ (dpm/100kg),
 239 dpm/100kg, Eq. 7a) and its associated uncertainty $(\sigma((A_{210Pb})_{spl,t_{spl}}))$ (dpm/100kg, Eq. 7b):

$$240 \quad (A_{210Pb})_{spl,t_{spl}} \left(\frac{dpm}{100kg}\right) = \frac{(A_{210Pb})_{spl,t_{spl}}}{m_{spl}} 100 \quad \text{Eq. 7a}$$

$$241 \quad \sigma\left((A_{210Pb})_{spl,t_{spl}} \left(\frac{dpm}{100kg}\right)\right) = \sqrt{\sigma\left((A_{210Pb})_{spl,t_{spl}}\right)^2 \left(\frac{100}{m_{spl}}\right)^2} \quad \text{Eq. 7b}$$

242

243 *Step B: Calculation of ^{210}Po activity and associated uncertainty in the sample*

244 Step B1: Calculation of ^{210}Po activity in the plating solution at the first plating date $((A_{210Po})_{sol,t_{plat1}})$, dpm,
 245 Eq. 8a) and its associated uncertainty $(\sigma((A_{210Po})_{sol,t_{plat1}}))$, dpm, Eq. 8b) after correction for detector
 246 background, Po recovery and ^{210}Po decay during counting and between the dates of first plating and the
 247 start of counting:

$$248 \quad (A_{210Po})_{sol,t_{plat1}} = \left(\frac{C_{210Po,1}}{T_{c1}} - (A_{210Po})_{bg,1} \right) \frac{\lambda_{210Po} T_{c1}}{1 - e^{-\lambda_{210Po} T_{c1}}} \frac{(A_{209Po})_{sp,t_{cal}} e^{-\lambda_{209Po}(t_{c1, st} - t_{sp, cal})} m_{sp1}}{\left(\frac{C_{209Po,1}}{T_{c1}} - (A_{209Po})_{bg,1} \right) \frac{\lambda_{209Po} T_{c1}}{1 - e^{-\lambda_{209Po} T_{c1}}}} e^{\lambda_{210Po}(t_{c1, st} - t_{plat1})}$$

249 *Eq. 8a*

$$250 \quad \sigma \left((A_{210Po})_{sol,t_{plat1}} \right) =$$

$$251 \quad \sqrt{\begin{aligned} & \sigma(C_{210Po,1})^2 \left(\frac{\lambda_{210Po}}{1 - e^{-\lambda_{210Po} T_{c1}}} \frac{(A_{209Po})_{sp,t_{cal}} e^{-\lambda_{209Po}(t_{c1, st} - t_{sp, cal})} m_{sp1}}{\left(\frac{C_{209Po,1}}{T_{c1}} - (A_{209Po})_{bg,1} \right) \frac{\lambda_{209Po} T_{c1}}{1 - e^{-\lambda_{209Po} T_{c1}}}} e^{\lambda_{210Po}(t_{c1, st} - t_{plat1})} \right)^2 \\ & + \sigma((A_{210Po})_{bg,1})^2 \left(\frac{\lambda_{210Po} T_{c1}}{1 - e^{-\lambda_{210Po} T_{c1}}} \frac{(A_{209Po})_{sp,t_{cal}} e^{-\lambda_{209Po}(t_{c1, st} - t_{sp, cal})} m_{sp1}}{\left(\frac{C_{209Po,1}}{T_{c1}} - (A_{209Po})_{bg,1} \right) \frac{\lambda_{209Po} T_{c1}}{1 - e^{-\lambda_{209Po} T_{c1}}}} e^{\lambda_{210Po}(t_{c1, st} - t_{plat1})} \right)^2 \\ & + \sigma((A_{209Po})_{sp,t_{cal}})^2 \left(\left(\frac{C_{210Po,1}}{T_{c1}} - (A_{210Po})_{bg,1} \right) \frac{\lambda_{210Po} T_{c1}}{1 - e^{-\lambda_{210Po} T_{c1}}} \frac{e^{-\lambda_{209Po}(t_{c1, st} - t_{sp, cal})} m_{sp1}}{\left(\frac{C_{209Po,1}}{T_{c1}} - (A_{209Po})_{bg,1} \right) \frac{\lambda_{209Po} T_{c1}}{1 - e^{-\lambda_{209Po} T_{c1}}}} e^{\lambda_{210Po}(t_{c1, st} - t_{plat1})} \right)^2 \\ & + \sigma(C_{209Po,1})^2 \left(\left(\frac{C_{210Po,1}}{T_{c1}} - (A_{210Po})_{bg,1} \right) \frac{\lambda_{210Po} T_{c1}}{1 - e^{-\lambda_{210Po} T_{c1}}} \frac{(A_{209Po})_{sp,t_{cal}} e^{-\lambda_{209Po}(t_{c1, st} - t_{sp, cal})} m_{sp1}}{(C_{209Po,1} - T_{c1} (A_{209Po})_{bg,1})^2 \frac{\lambda_{209Po}}{1 - e^{-\lambda_{209Po} T_{c1}}}} e^{\lambda_{210Po}(t_{c1, st} - t_{plat1})} \right)^2 \\ & + \sigma((A_{209Po})_{bg,1})^2 \left(\left(\frac{C_{210Po,1}}{T_{c1}} - (A_{210Po})_{bg,1} \right) \frac{\lambda_{210Po} T_{c1}}{1 - e^{-\lambda_{210Po} T_{c1}}} \frac{(A_{209Po})_{sp,t_{cal}} e^{-\lambda_{209Po}(t_{c1, st} - t_{sp, cal})} m_{sp1} T_{c1}}{(C_{209Po,1} - T_{c1} (A_{209Po})_{bg,1})^2 \frac{\lambda_{209Po}}{1 - e^{-\lambda_{209Po} T_{c1}}}} e^{\lambda_{210Po}(t_{c1, st} - t_{plat1})} \right)^2 \end{aligned}}$$

252 *Eq. 8b*

253

254 Step B2: Calculation of ^{210}Po activity in the plating solution at the date of extraction (dissolved or total
255 samples) or dissolution (particulate samples) $((A_{210Po})_{sol,t_{extr}}$, dpm, Eq. 9a) and its associated uncertainty
256 $(\sigma((A_{210Po})_{sol,t_{extr}}$, dpm, Eq. 9b) after correction for ^{210}Po decay and in-growth between extraction and first
257 plating dates:

$$259 \quad (A_{210Po})_{sol,t_{extr}}$$

$$260 \quad = \left((A_{210Po})_{sol,t_{plat1}} - \frac{\lambda_{210Po} \left((A_{210Pb})_{spl,t_{spl}} e^{-\lambda_{210Pb}(t_{extr} - t_{spl})} + (A_{210Pb})_B e^{-\lambda_{210Pb}(t_{extr} - t_{car})} \right) f_{Pbrec1}}{\lambda_{210Po} - \lambda_{210Pb}} \left(e^{-\lambda_{210Pb}(t_{plat1} - t_{extr})} \right. \right.$$

$$261 \quad \left. - e^{-\lambda_{210Po}(t_{plat1} - t_{extr})} \right) e^{\lambda_{210Po}(t_{plat1} - t_{extr})}$$

258 *Eq. 9a*

262

263

$$\sigma((A_{210Po})_{sol,t_{extr}}) =$$

264

$$\sqrt{\begin{aligned} & \sigma((A_{210Po})_{sol,t_{plat1}})^2 (e^{\lambda_{210Po}(t_{plat1}-t_{extr})})^2 \\ & + \sigma((A_{210Pb})_{spl,t_{spl}})^2 \left(\frac{\lambda_{210Po} e^{-\lambda_{210Pb}(t_{extr}-t_{spl})} f_{Pb_{rec1}}}{\lambda_{210Po} - \lambda_{210Pb}} (e^{-\lambda_{210Pb}(t_{plat1}-t_{extr})} - e^{-\lambda_{210Po}(t_{plat1}-t_{extr})}) e^{\lambda_{210Po}(t_{plat1}-t_{extr})} \right)^2 \\ & + \sigma((A_{210Pb})_B)^2 \left(\frac{\lambda_{210Po} e^{-\lambda_{210Pb}(t_{extr}-t_{car})} f_{Pb_{rec1}}}{\lambda_{210Po} - \lambda_{210Pb}} (e^{-\lambda_{210Pb}(t_{plat1}-t_{extr})} - e^{-\lambda_{210Po}(t_{plat1}-t_{extr})}) e^{\lambda_{210Po}(t_{plat1}-t_{extr})} \right)^2 \\ & + \sigma(f_{Pb_{rec1}})^2 \left(\frac{\lambda_{210Po} ((A_{210Pb})_{spl,t_{spl}} e^{-\lambda_{210Pb}(t_{extr}-t_{spl})} + (A_{210Pb})_B e^{-\lambda_{210Pb}(t_{extr}-t_{car})})}{\lambda_{210Po} - \lambda_{210Pb}} \right)^2 \\ & \left(e^{-\lambda_{210Pb}(t_{plat1}-t_{extr})} - e^{-\lambda_{210Po}(t_{plat1}-t_{extr})} \right) e^{\lambda_{210Po}(t_{plat1}-t_{extr})} \end{aligned}}$$

265

Eq. 9b

266

267

$f_{Pb_{rec1}}$ and its associated uncertainty $\sigma(f_{Pb_{rec1}})$ represents the Pb recovery efficiency during sample extraction

268

(filtered or unfiltered samples). It is obtained by :

269

$$f_{Pb_{rec1}} = \frac{m_{sol1}[Pb]_{sol1}}{m_c[Pb]_c} \quad Eq. 10a$$

270

$$\sigma(f_{Pb_{rec1}}) = \sqrt{\sigma([Pb]_{sol1})^2 \left(\frac{m_{sol1}}{m_c[Pb]_c} \right)^2 + \sigma([Pb]_c)^2 \left(\frac{m_{sol1}[Pb]_{sol1}}{m_c[Pb]_c^2} \right)^2} \quad Eq. 10b$$

271

272

Note that for particulate samples, the date of extraction (t_{extr}) in Eq. 9a and Eq. 9b should be replaced by

273

the date of dissolution (t_{diss}), assuming that any loss of Pb that occurs during particulate sample processing

274

is during the dissolution procedure.

275

276

Step B3: Calculation of ^{210}Po activity in the sample at sampling date ($(A_{210Po})_{sol,t_{spl}}$, dpm, Eq. 11a) and its

277

associated uncertainty ($\sigma((A_{210Po})_{sol,t_{spl}})$, dpm, Eq. 11b) after correction for the blank and for ^{210}Po decay

278

and in-growth between sampling date and extraction (dissolved or total) or dissolution (particulate) dates:

$$\begin{aligned}
280 \quad (A_{210Po})_{spl,t_{spl}} &= (A_{210Po})_{sol,t_{extr}} e^{\lambda_{210Po}(t_{extr}-t_{spl})} \\
281 \quad &- \frac{\lambda_{210Po}(A_{210Pb})_{spl,t_{spl}}}{\lambda_{210Po} - \lambda_{210Pb}} \left(e^{-\lambda_{210Pb}(t_{extr}-t_{spl})} - e^{-\lambda_{210Po}(t_{extr}-t_{spl})} \right) e^{\lambda_{210Po}(t_{extr}-t_{spl})} \\
282 \quad &- \frac{\lambda_{210Po}(A_{210Pb})_B}{\lambda_{210Po} - \lambda_{210Pb}} \left(e^{-\lambda_{210Pb}(t_{extr}-t_{car})} - e^{-\lambda_{210Po}(t_{extr}-t_{car})} \right) e^{\lambda_{210Po}(t_{extr}-t_{car})} - (A_{210Po})_B \\
279 \quad & \hspace{15em} Eq. 11a
\end{aligned}$$

$$\begin{aligned}
284 \quad & \sigma \left((A_{210Po})_{spl,t_{spl}} \right) \\
285 \quad &= \sqrt{ \begin{aligned} & \sigma \left((A_{210Po})_{sol,t_{extr}} \right)^2 \left(e^{\lambda_{210Po}(t_{extr}-t_{spl})} \right)^2 \\ & + \sigma \left((A_{210Pb})_{spl,t_{spl}} \right)^2 \left(\frac{\lambda_{210Po}}{\lambda_{210Po} - \lambda_{210Pb}} \left(e^{-\lambda_{210Pb}(t_{extr}-t_{spl})} - e^{-\lambda_{210Po}(t_{extr}-t_{spl})} \right) e^{\lambda_{210Po}(t_{extr}-t_{spl})} \right)^2 \\ & + \sigma \left((A_{210Pb})_B \right)^2 \left(\frac{\lambda_{210Po}}{\lambda_{210Po} - \lambda_{210Pb}} \left(e^{-\lambda_{210Pb}(t_{extr}-t_{car})} - e^{-\lambda_{210Po}(t_{extr}-t_{car})} \right) e^{\lambda_{210Po}(t_{extr}-t_{car})} \right)^2 \\ & + \sigma \left((A_{210Po})_B \right)^2 \end{aligned} } \\
283 \quad & \hspace{15em} Eq. 11b
\end{aligned}$$

286

287 In the case of particulate samples, t_{extr} should be replaced by t_{diss} in Eq. 11a and Eq. 11b.

288

289 The parameters $(A_{210Po})_B$ and $\sigma((A_{210Po})_B)$ correspond to the activity and its associated uncertainty,
290 respectively, of ^{210}Po in the blank, which should be obtained by processing a volume of ultrapure water
291 using the same reagents as would a sample, according to the procedure outlined in Figure 1. They are
292 calculated following step B1 and by replacing the equations of step B2 by:

$$\begin{aligned}
293 \quad (A_{210Po})_B &= (A_{210Po})_{sol,t_{plat1}} e^{\lambda_{210Po}(t_{plat1}-t_{car})} \\
294 \quad &- \frac{\lambda_{210Po}(A_{210Pb})_B e^{-\lambda_{210Pb}(t_{extr}-t_{car})} f_{Pbrec1}}{\lambda_{210Po} - \lambda_{210Pb}} \left(e^{-\lambda_{210Pb}(t_{plat1}-t_{extr})} \right. \\
295 \quad & \left. - e^{-\lambda_{210Po}(t_{plat1}-t_{extr})} \right) e^{\lambda_{210Po}(t_{plat1}-t_{extr})} \\
296 \quad &- \frac{\lambda_{210Po}(A_{210Pb})_B}{\lambda_{210Po} - \lambda_{210Pb}} \left(e^{-\lambda_{210Pb}(t_{extr}-t_{car})} - e^{-\lambda_{210Po}(t_{extr}-t_{car})} \right) e^{\lambda_{210Po}(t_{extr}-t_{car})} \\
297 \quad & \hspace{15em} Eq. 12a
\end{aligned}$$

298

$$\sigma((A_{210Po})_B) =$$

$$\begin{aligned}
 & \sqrt{ \sigma((A_{210Po})_{sol,t_{plat1}})^2 (e^{\lambda_{210Po}(t_{plat1}-t_{car})})^2 } \\
 & + \sigma((A_{210Pb})_B)^2 \left(\frac{\lambda_{210Po} e^{-\lambda_{210Pb}(t_{extr}-t_{car})} f_{Pb_{rec1}}}{\lambda_{210Po} - \lambda_{210Pb}} (e^{-\lambda_{210Pb}(t_{plat1}-t_{extr})} - e^{-\lambda_{210Po}(t_{plat1}-t_{extr})}) e^{\lambda_{210Po}(t_{plat1}-t_{extr})} \right)^2 \\
 & + \sigma((A_{210Pb})_B)^2 \left(\frac{\lambda_{210Po}}{\lambda_{210Po} - \lambda_{210Pb}} (e^{-\lambda_{210Pb}(t_{extr}-t_{car})} - e^{-\lambda_{210Po}(t_{extr}-t_{car})}) e^{\lambda_{210Po}(t_{extr}-t_{car})} \right)^2 \\
 & + \sigma(f_{Pb_{rec1}})^2 \left(\frac{\lambda_{210Po} (A_{210Pb})_B e^{-\lambda_{210Pb}(t_{extr}-t_{car})}}{\lambda_{210Po} - \lambda_{210Pb}} (e^{-\lambda_{210Pb}(t_{plat1}-t_{extr})} - e^{-\lambda_{210Po}(t_{plat1}-t_{extr})}) e^{\lambda_{210Po}(t_{plat1}-t_{extr})} \right)^2
 \end{aligned}$$

299

Eq. 12b

300

301 Step B4: Final calculation of ^{210}Po activity in the sample at the sampling date $((A_{210Po})_{spl,t_{spl}}$ (dpm/100kg)),302 dpm/100kg, Eq. 13a) and its associated uncertainty $(\sigma((A_{210Po})_{spl,t_{spl}}$ (dpm/100kg)), dpm/100kg, Eq. 13b):

$$303 \quad (A_{210Po})_{spl,t_{spl}} \left(\frac{dpm}{100kg} \right) = \frac{(A_{210Po})_{spl,t_{spl}}}{m_{spl}} 100 \quad \text{Eq. 13a}$$

$$304 \quad \sigma \left((A_{210Po})_{spl,t_{spl}} \left(\frac{dpm}{100kg} \right) \right) = \sqrt{ \sigma \left((A_{210Po})_{spl,t_{spl}} \right)^2 \left(\frac{100}{m_{spl}} \right)^2 } \quad \text{Eq. 13b}$$

305

306 *Step C: Calculation of the $^{210}\text{Po}/^{210}\text{Pb}$ activity ratio and associated uncertainty in the sample*307 The final $^{210}\text{Po}/^{210}\text{Pb}$ activity ratio in the sample at the sampling date $\left(\frac{(A_{210Po})_{spl,t_{spl}}}{(A_{210Pb})_{spl,t_{spl}}} \right)$ is simply obtained by308 dividing $(A_{210Po})_{spl,t_{spl}}$ (Eq. 11a) by $(A_{210Pb})_{spl,t_{spl}}$ (Eq. 4a). Its associated uncertainty $\left(\sigma \left(\frac{(A_{210Po})_{spl,t_{spl}}}{(A_{210Pb})_{spl,t_{spl}}} \right) \right)$ can be309 obtained using Eq. 14b. Note that Eq. 14b is only valid if the same ^{209}Po spike is used in steps A and B and

310 should be adapted if otherwise. Note also that for simplicity, influence of the blank in Eq. 14b was neglected.

311

312

313

319

320 **Discussion**

321 *Influence of the relative uncertainty of individual parameters on the final ^{210}Po , ^{210}Pb and $^{210}\text{Po}/^{210}\text{Pb}$*
322 *uncertainties*

323 The main sources of uncertainty detailed in the previous calculations are: (1) the number of counts
324 for ^{210}Po ($C_{210\text{Po},1}$ and $C_{210\text{Po},2}$) and ^{209}Po ($C_{209\text{Po},1}$ and $C_{209\text{Po},2}$) detected by alpha spectrometry, (2) the
325 activity of ^{209}Po in the spike ($(A_{209\text{Po}})_{sp,ical}$), (3) the detector background for each isotope ($(A_{210\text{Po}})_{bg}$ and
326 $(A_{209\text{Po}})_{bg}$) and (4) the estimated Pb recovery from sample processing ($f_{\text{Pb},rec1}$ and $f_{\text{Pb},rec,tot}$). For ^{210}Po , a fifth
327 source of uncertainty needs to be considered that includes the error associated with ^{210}Pb , since it is used in
328 the calculation to correct for ^{210}Po ingrowth during sample processing (i.e., Eq. 9 and Eq. 11). In this
329 section, we report the relative influence each source of error has on the cumulative uncertainty of ^{210}Po
330 and ^{210}Pb activities and the $^{210}\text{Po}/^{210}\text{Pb}$ activity ratio for typical experimental and environmental
331 conditions.

332 The influence of a specific parameter's uncertainty on the overall uncertainty of ^{210}Po and ^{210}Pb
333 activity, as well as the $^{210}\text{Po}/^{210}\text{Pb}$ activity ratio, is dependent on two factors: (1) the relative uncertainty of
334 all parameters considered in the calculations, and (2) the relative weight that each parameter has in the
335 final calculated activity. The relative uncertainty of each parameter (factor 1) is only dependent on
336 individual experimental conditions. These include uncertainty of the spike calibration for spike activity,
337 counting statistics for ^{209}Po and ^{210}Po in the sample and during background measurements, and on the
338 analysis of stable Pb concentrations in the aliquots used for determining the recovery. In contrast, the
339 relative weight of each parameter's uncertainty on the final calculated activity (factor 2) is dependent on
340 the uncertainty calculations obtained by error propagation. These need to be precisely estimated in order to
341 identify which parameter listed above has the most influence on the uncertainty of the final results and
342 therefore, will provide information on areas where additional effort is needed.

343 We estimated the influence of the relative uncertainty of each parameter on the final calculated
344 ^{210}Po and ^{210}Pb activities and $^{210}\text{Po}/^{210}\text{Pb}$ activity ratio based on the data obtained from ~ 200 dissolved

345 (<0.2 μm), particulate (>1 μm) and total (unfiltered) seawater samples collected from the North Atlantic
346 and Pacific Oceans during GEOTRACES transects (GA-02 and GA-03) and inter-calibration cruises
347 (Church et al. 2012). The range of values for the parameters considered within this large database (Table
348 2) is expected to reflect the typical range of experimental and environmental conditions that are
349 encountered during most ^{210}Po and ^{210}Pb determinations. The influence of each parameter was tested
350 separately (i.e.; one at a time), by using the equations presented previously and forcing the relative
351 uncertainty of the parameter of interest to vary from 0 to 15% (range of possible values) while fixing the
352 relative uncertainty of the other parameters at 0%. Please note that the relative uncertainty of each
353 parameter is defined to be similar between the two steps of sample processing (Steps A: ^{210}Pb
354 determination; Steps B: ^{210}Po determination).

355 Results are reported in Figure 3. Among the tested parameters, those that have the most important
356 influence on the final uncertainty of both *in situ* ^{210}Po and ^{210}Pb activities are: (1) the calibrated ^{209}Po
357 activity in the spike, (2) the number of counts of ^{210}Po and ^{209}Po detected by alpha spectrometry, and (3)
358 the Pb recovery efficiency (Figure 3). The uncertainty on the number of counts of ^{210}Po and ^{209}Po and the
359 Pb recovery efficiency has also an important influence on the final uncertainty of $^{210}\text{Po}/^{210}\text{Pb}$ activity ratio.
360 However, it is worth noting that the uncertainty on the spike activity does not impact the final uncertainty
361 of $^{210}\text{Po}/^{210}\text{Pb}$ activity ratio as such parameter cancel out in the $^{210}\text{Po}/^{210}\text{Pb}$ uncertainty calculation (Eq.
362 14b). Note that such observation is only valid if the same ^{209}Po spike is used between both steps A and B.
363 In the case of ^{210}Po , the ^{210}Pb uncertainty also has an important influence on the final relative uncertainty
364 (Figure 4). In contrast, the uncertainties associated with the detector backgrounds have a significantly
365 lower influence on the final calculated ^{210}Po and ^{210}Pb activities and the $^{210}\text{Po}/^{210}\text{Pb}$ activity ratio (Figure
366 3). It is worth noting that, for the dataset considered, the detector backgrounds were always <5% of the
367 ^{210}Po and ^{209}Po activities detected by individual alpha detectors.

368
369 ***Influence of the ^{210}Po and ^{210}Pb activities in blanks on the final ^{210}Po and ^{210}Pb activities and associated***
370 ***uncertainties***

371 Reagents used during sample processing may be contaminated with ^{210}Po and ^{210}Pb and impact the
372 final ^{210}Po and ^{210}Pb activities and $^{210}\text{Po}/^{210}\text{Pb}$ activity ratios as well as their respective uncertainties. One of
373 the most important sources of contamination is the Pb carrier solution, which can contain significant
374 amounts of ^{210}Po and ^{210}Pb (e.g., [Baskaran et al., 2013](#)). Based on the dataset from the typical experimental
375 and environmental conditions stated above, we evaluate the influence of blank contamination by varying
376 the ^{210}Po and ^{210}Pb activities in blanks between 0.00 and 0.10 dpm and assuming radioactive equilibrium
377 between the two nuclides in blanks (Figure 5). The increase of ^{210}Po and ^{210}Pb activities in the blank results
378 in, as expected, a decrease in the final activity on ^{210}Po and ^{210}Pb , with ^{210}Pb slightly higher than ^{210}Po . As
379 such, it also induces a slight increase, on average, of the $^{210}\text{Po}/^{210}\text{Pb}$ activity ratio that can however induce
380 up to 20% variation for the highest blank activity tested (Figure 5). This clearly highlights the importance
381 of evaluating the blank contamination and to include it in the calculations.

382

383 ***Implications for the final uncertainty on ^{210}Po and ^{210}Pb activities and $^{210}\text{Po}/^{210}\text{Pb}$ activity ratios***

384 In order to use ^{210}Po and ^{210}Pb as quantitative tracers for particles dynamic modeling in the ocean,
385 the determination in seawater samples should be as precise as possible (i.e., their relative uncertainty
386 should be as low as possible). In practice, the lowest relative uncertainties are assumed to be 3% for the
387 ^{209}Po spike calibration, 3.5% for counting statistics and 3% for the Pb recovery and ^{210}Po and ^{210}Pb
388 activities in the blank can be considered negligible (see next section). By applying these relative
389 uncertainties to the typical experimental and environmental conditions stated above, the mean relative
390 uncertainties on ^{210}Po and ^{210}Pb activities and the $^{210}\text{Po}/^{210}\text{Pb}$ activity ratio that can be obtained are $11 \pm$
391 6% , $7.4 \pm 0.4\%$ and $14 \pm 7\%$, respectively. Such relative uncertainties may be considered acceptable for
392 oceanic process modeling for ^{210}Pb . However, the higher and more variable relative uncertainties on the
393 final calculated ^{210}Po and the $^{210}\text{Po}/^{210}\text{Pb}$ activity ratios is due to the fact that they incorporate the
394 uncertainty of the final calculated ^{210}Pb from the ingrowth correction (cf., Eq. 9b and Eq. 11b). The extent
395 of such a correction depends on two factors: (1) the $^{210}\text{Po}/^{210}\text{Pb}$ activity ratio in the sample (the lower the
396 ratio, the higher the correction) and (2) the time elapsed between the sampling and the first Po plating (the

397 longer the time elapsed, the higher the correction). The lowest ^{210}Po relative uncertainty obtainable for the
398 experimental conditions described is 6%, and then only obtained for those samples with a high $^{210}\text{Po}/^{210}\text{Pb}$
399 ratio (≥ 1) and the shortest delay between sampling and sample processing (< 80 days) (Figure 6).

400 Variations in sample characteristics (e.g., $^{210}\text{Po}/^{210}\text{Pb}$ activity ratio) and experimental conditions (e.g., time
401 elapsed between sampling and first plating) can thus explain the high variability in the relative uncertainty
402 obtained for ^{210}Po .

403

404 **Comments and Recommendations**

405 *Limitation of uncertainties on in situ ^{210}Po , ^{210}Pb and $^{210}\text{Po}/^{210}\text{Pb}$ determinations*

406 We previously identified the main sources of uncertainty in the ^{210}Po and ^{210}Pb determination. If
407 there is no way to modify the $^{210}\text{Po}/^{210}\text{Pb}$ activity ratio in the sample, there are however several other ways
408 to reduce the extent of the uncertainty for both ^{210}Po and ^{210}Pb and therefore $^{210}\text{Po}/^{210}\text{Pb}$ activity ratios.

409

410 *Time between sampling and first plating*

411 As the delay between the sampling and the first plating increases, the uncertainty on the ^{210}Po also
412 increases. Therefore, it is imperative to process samples as soon as possible after collection. However, it is
413 not always possible to practically limit this delay. This is particularly the case when considering long
414 sampling cruises. For typical seawater samples and the experimental conditions presented previously, a
415 delay of 3 months from time of collection at sea to first plating ashore will induce a relative uncertainty on
416 ^{210}Po of about 7% ($^{210}\text{Po}/^{210}\text{Pb}$ activity ratio > 2), 9% ($^{210}\text{Po}/^{210}\text{Pb}$ activity ratio ~ 1) and 13% ($^{210}\text{Po}/^{210}\text{Pb}$
417 activity ratio ~ 0.5) (Figure 6b). In comparison, those uncertainties would be reduced to about 6% for
418 sample processed onboard and plated within a few days after collection. Onboard processing of samples,
419 including precipitation, filtration, dissolution/digestion and plating requires the use of specific equipment
420 (e.g., chemical fume hoods). As research vessels continue to become more modernized, we recommend
421 that such processing to be done onboard in order to minimize the impact of the needed corrections.

422

423 *Counting statistics*

424 One of the largest sources of uncertainty is that associated with the number of ^{210}Po and ^{209}Po
425 counts by alpha spectrometry. The uncertainty on counting is calculated using the square root of the
426 number of counts (e.g., Ludwig 2003), thus, the relative uncertainty on counting results decrease with an
427 increase in the number of counts following a $y=x^{1/2}/x$ shaped-curve. Consequently, it is relatively easy to
428 decrease this uncertainty by increasing the counting time, assuming detector backgrounds are relatively
429 minor. For practical reasons, however, it is also necessary to balance counting periods with the number of
430 samples that needs to be measured and counter availability. For an acceptable relative uncertainty $<3.5\%$,
431 a minimum of ~ 820 counts is needed. For ^{210}Po , this can be obtained for a 10L dissolved seawater sample
432 with a ^{210}Po activity of $15 \text{ dpm} \cdot 100\text{L}^{-1}$, assuming a Po recovery of 80% and a detector efficiency of 15%,
433 in about 3 days of counting.

434

435 *Spike calibration*

436 The reported ^{209}Po activity in commercial stock solutions, from which ^{209}Po spikes are generally
437 made, is typically certified with a relative uncertainty $< 5\%$ (e.g., a ^{209}Po solution from Eckert & Ziegler is
438 certified at 3.1%; www.ezag.com). For the typical experimental and environmental conditions stated
439 above, such an uncertainty can impart a 5% relative uncertainty for ^{210}Pb final activities and as much as
440 20% for ^{210}Po activities (Figure 3). Since the spike solution activity can vary with storage (e.g., due to
441 evaporation) and because of the relatively high uncertainty on the ^{209}Po decay constant ($102 \pm 5\text{y}$), we
442 recommend a regular calibration of the spike over time. Such calibrations imply the use of ^{210}Po certified
443 standards. The use of IAEA standard RGU-1 (IAEA 1987) is recommended for such calibrations due to its
444 low relative uncertainty on the ^{210}Po activity ($<1\%$). We also recommend the use of the same ^{209}Po spike
445 during sample processing as it allows to significantly decrease the uncertainty on $^{210}\text{Po}/^{210}\text{Pb}$ activity
446 ratios.

447

448 *Pb recovery efficiency*

449 The uncertainty associated with Pb recoveries is essentially dependent on that associated with the
450 determination of stable Pb concentrations in the aliquots and carrier solution (Eq. 6b and Eq. 7b) as
451 obtained by routine analytical techniques (e.g., atomic absorption spectrometry, [Fleer and Bacon 1984](#);
452 [Friedrich and Rutgers van der Loeff 2002](#)). In order to reduce the uncertainty associated with this analysis,
453 we recommend adding an amount of stable Pb to samples in sufficient quantity to ensure accurate
454 standardization. For example, an addition of ~10 mg of Pb into the sample easily allows the Pb
455 concentration to be determined by flame atomic absorption spectrometry (or ICPMS) with a relative
456 uncertainty $\leq 3\%$, as this will result in Pb concentrations ranging from 5 to 15 $\mu\text{g g}^{-1}$ in a 20 times diluted
457 10 ml plating solution assuming a 70-95% total Pb extraction efficiency.

458

459 *Blank consideration*

460 We showed that the blank could strongly impact the ^{210}Po and ^{210}Pb activities and the $^{210}\text{Po}/^{210}\text{Pb}$
461 activity ratios and thus could induce an increase of their associated uncertainties. However, this essentially
462 depends on the purity of the reagents used. One of the main sources of contamination for ^{210}Po and ^{210}Pb is
463 the Pb carrier, which can contain significant amount of both isotopes. In order to minimize the blank, it is
464 recommended that the carrier be made using lead obtained from ancient sources (i.e., >200y) or pure
465 galena mineral that was shown to present the lowest ^{210}Pb activity ([Cochran et al., 1983](#)).

466

467 **Summary**

468 This paper presents methodologies for improving accuracy and precision in the determination of
469 ^{210}Po and ^{210}Pb activities in seawater samples. This will allow one to compare data reported by different
470 labs, and to use this isotope pair as a quantitative tracer for particle dynamics in marine systems.

471 First, we recommend that the accuracy of the method can be significantly improved by: (1)
472 systematic use of ion exchange resin for Po removal after the first plating, (2) accounting for recovery of
473 ^{210}Pb during both extraction/dissolution and ion exchange resin separation steps, (3) use of Pb yield tracer
474 made from sufficiently old lead material (>hundred of years) or lead old mineral (e.g., galena) and (4) use

475 of appropriate calculations for decay/ingrowth, recovery and blank corrections, as detailed herein. We also
476 provide as downloadable Web Appendix a spread-sheet outlining these calculations.

477 Second, the overall precision of the methodology is discussed by evaluating the impact of the
478 relative uncertainty on each individual parameter included in the calculations. Parameters that have the
479 most important influence on the final uncertainty of both *in situ* ^{210}Po and ^{210}Pb activities and thus the
480 $^{210}\text{Po}/^{210}\text{Pb}$ activity ratio are: (1) the calibrated ^{209}Po activity in the spike, (2) the number of counts of ^{210}Po
481 and ^{209}Po detected by alpha spectrometry, and (3) the Pb recovery efficiency. Blank contamination was
482 also showed to increase the final relative uncertainty on ^{210}Po , ^{210}Pb and $^{210}\text{Po}/^{210}\text{Pb}$. For typical
483 experimental and environmental conditions, such relative uncertainties are about 7% for ^{210}Pb . However,
484 uncertainties can be considerably larger (up to 35%) for ^{210}Po , particularly for samples with low (<1)
485 $^{210}\text{Po}/^{210}\text{Pb}$ activity ratios and when there is a long delay (>80 d) between sampling and the first Po plating.
486 In contrast, for higher $^{210}\text{Po}/^{210}\text{Pb}$ activity ratios and shorter delays between sample collection and
487 processing, the method described herein allows determination of the ^{210}Po activity within a 6% relative
488 uncertainty.

489

490

491 **References**

- 492 Bacon, M. P., D. W. Spencer, and P. G. Brewer. 1976. $^{210}\text{Pb}/^{226}\text{Ra}$ and $^{210}\text{Po}/^{210}\text{Pb}$ disequilibria in
493 seawater and suspended particulate matter. *Earth Planet. Sci. Lett.* **32**: 277-296.
- 494 Baskaran, M., T. M. Church, G. Hong, A. Kumar, M. Qiang, H.-Y. Choi, S. Rigaud and K. Maiti. 2013.
495 Effects of flow rates and composition of the filter, and decay/ingrowth correction factors involved
496 with the determination of in situ particulate ^{210}Po and ^{210}Pb in seawater. *Limnol. Oceanogr. Meth.*
497 **11**:126-138.
- 498 Bojanowski, R., R. Fukai, S. Ballestra, and H. Asari. 1983. Determination of natural radioactive elements
499 in marine environmental materials by ion exchange and alpha spectrometry, p. 1-13. *In* I.A.E.A.
500 [ed.].
- 501 Church, T. M., S. Rigaud, M. Baskaran, A. Kumar, J. Friedrich, P. Masqué, V. Puigcorbé, G. Kim, O.
502 Radakovitch, G. Hong, H.-Y. Choi, and G. Stewart. 2012. Inter-calibration studies of ^{210}Po and
503 ^{210}Pb in dissolved and particulate sea water samples. *Limnol. Oceanogr. Meth.* **10**:776-789.
- 504 Cochran, J. K., and P. Masqué. 2003. Short-lived U/Th Series Radionuclides in the Ocean: Tracers for
505 Scavenging Rates, Export Fluxes and Particle Dynamics. *Rev. Mineral. Geochem.* **52**: 461-492.
- 506 Cochran, J. K., M. P. Bacon, S. Krishnaswami, and K. K. Turekian. 1983. ^{210}Po and ^{210}Pb distributions
507 in the central and eastern Indian Ocean. *Earth and Planetary Science Letters* **65**: 433-452.
- 508 Fler, A. P., and M. P. Bacon. 1984. Determination of ^{210}Pb and ^{210}Po in seawater and marine
509 particulate matter. *Nucl. Instrum. Methods Phys. Res.* **223**: 243-249.
- 510 Flynn, W. W. 1968. The determination of low levels of polonium-210 in environmental materials. *Anal.*
511 *Chim. Acta* **43**: 221-227.
- 512 Friedrich, J., and M. M. Rutgers Van Der Loeff. 2002. A two-tracer (^{210}Po - ^{234}Th) approach to
513 distinguish organic carbon and biogenic silica export flux in the Antarctic Circumpolar Current.
514 *Deep-Sea Res. PT I* **49**: 101-120.
- 515 IAEA. 1987. Preparation and certification of IAEA gamma-ray spectrometry and reference materials

516 RGU-1, RGTh-1 and RGK-1, p. 48. *In* I. A. E. Agency [ed.], Technical Report IAEA/RL/148.

517 Ludwig, K. R. 2003. Mathematical–Statistical Treatment of Data and Errors for ²³⁰Th/U Geochronology.

518 *Rev. Mineral. Geochem.* **52**: 631-656.

519 Masqué, P. and others 2002. Sediment accumulation rates and carbon fluxes to bottom sediments at the

520 Western Bransfield Strait (Antarctica). *Deep Sea Research Part II: Topical Studies in*

521 *Oceanography* **49**: 921-933.

522 Moore, W. S., and J. Dymondt. 1988. Correlation of ²¹⁰Pb removal with organic carbon fluxes in the

523 Pacific Ocean. *Nature* **331**: 339-341.

524 Nozaki, Y. 1986. ²²⁶Ra-²²²Rn-²¹⁰Pb systematics in seawater near the bottom of the ocean. *Earth Planet.*

525 *Sci. Lett.* **80**: 36-40.

526 Nozaki, Y., J. Thomson, and K. K. Turekian. 1976. The distribution of ²¹⁰Pb and ²¹⁰Po in the surface

527 waters of the Pacific Ocean. *Earth Planet. Sci. Lett.* **32**: 304-312.

528 Rutgers Van Der Loeff, M. M., and W. Geibert. 2008. Chapter 7 U- and Th-Series Nuclides as Tracers of

529 Particle Dynamics, Scavenging and Biogeochemical Cycles in the Oceans, p. 227-268. *In* S.

530 Krishnaswami and J. K. Cochran [eds.], *Radioactivity in the Environment*. Elsevier.

531 Rutgers van Der Loeff, M. M., and W. S. Moore. 2007. Determination of natural radioactive tracers, p.

532 365-397. *Methods of Seawater Analysis*. Wiley-VCH Verlag GmbH.

533 Sarin, M. M., R. Bhushan, R. Rengarajan, and D. N. Yadav. 1992. The simultaneous determination of

534 ²³⁸U series nuclides in seawater: results from the Arabian Sea and Bay of Bengal. *Indian J. Mar.*

535 *Sci.* **21**: 121-127.

536 Sarin, M. M., G. Kim, and T. M. Church. 1999. ²¹⁰Po and ²¹⁰Pb in the South-equatorial Atlantic:

537 distribution and disequilibrium in the Upper 500m. *Deep-Sea Res. PT II* **46**: 907-917.

538 Stewart, G. M., and N. S. Fisher. 2003. Experimental studies on the accumulation of polonium-210 by

539 marine phytoplankton. *Limnol. Oceanogr.* **48**: 9.

540 ---. 2003. Bioaccumulation of Polonium-210 in Marine Copepods. *Limnol. Oceanogr.* **48**: 2011-2019.

541 Stewart, G. M., S. W. Fowler, J.-L. Teyssie, O. Cotret, J. K. Cochran, and N. S. Fisher. 2005. Contrasting

542 transfer of polonium-210 and lead-210 across three trophic levels in marine plankton. *Mar. Ecol.*
543 *Prog. Ser.* **290**: 7.

544 Stewart, G. and others 2007. Comparing POC export from $^{234}\text{Th}/^{238}\text{U}$ and $^{210}\text{Po}/^{210}\text{Pb}$ disequilibria
545 with estimates from sediment traps in the northwest Mediterranean. *Deep-Sea Res. PT I* **54**:
546 1549-1570.

547 Thomson, J., and K. K. Turekian. 1976. ^{210}Po and ^{210}Pb distributions in ocean water profiles from the
548 Eastern South Pacific. *Earth Planet. Sci. Lett.* **32**: 297-303.

549 Tokieda, T., H. Narita, K. Harada, and S. Tsunogai. 1994. Sequential and rapid determination of Po-210,
550 Bi-210 and Pb-210 in natural waters. *Talanta* **41**: 2079-2085.

551 Vajda, N., J. Larosa, R. Zeisler, P. Danesi, and G. Kis-Benedek. 1997. A novel technique for the
552 simultaneous determination of ^{210}Pb and ^{210}Po using a crown ether. *J. Environ. Radioact.* **37**:
553 355-372.

554 Verdeny, E., P. Masqué, J. Garcia-Orellana, C. Hanfland, J. Kirk Cochran, and G. M. Stewart. 2009. POC
555 export from ocean surface waters by means of $^{234}\text{Th}/^{238}\text{U}$ and $^{210}\text{Po}/^{210}\text{Pb}$ disequilibria: A
556 review of the use of two radiotracer pairs. *Deep-Sea Res. PT II* **56**: 1502-1518.

557 Yang, W. F., Y. P. Huang, M. Chen, Y. S. Qiu, H. B. Li, and L. Zhang. 2011. Carbon and nitrogen
558 cycling in the Zhubi coral reef lagoon of the South China Sea as revealed by ^{210}Po and ^{210}Pb .
559 *Mar. Pollut. Bull.* **62**: 905-911.

560

Figures and Figure Legends

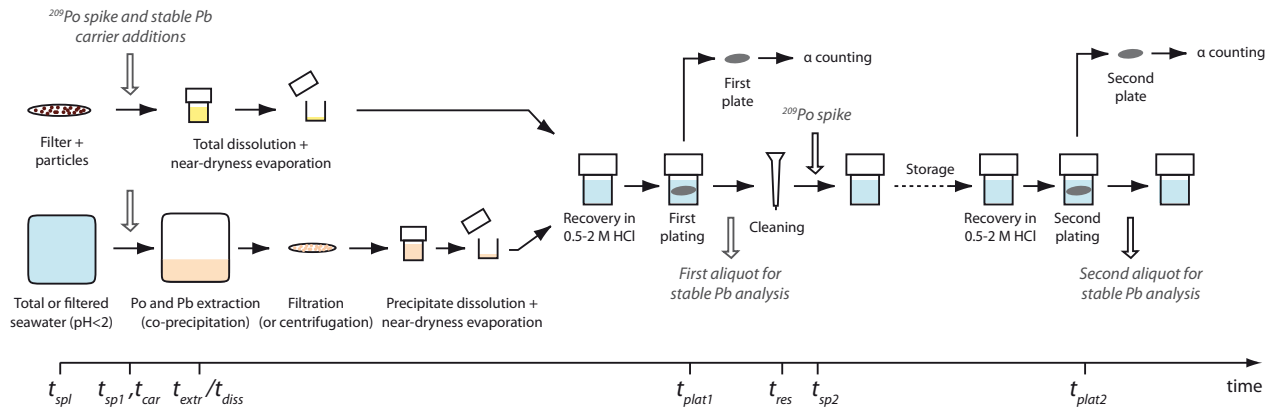


Figure 1: Sample processing scheme for the determination of total, dissolved and particulate ^{210}Po and ^{210}Pb activities. The times term (t) required for each step used in the calculation are provided.

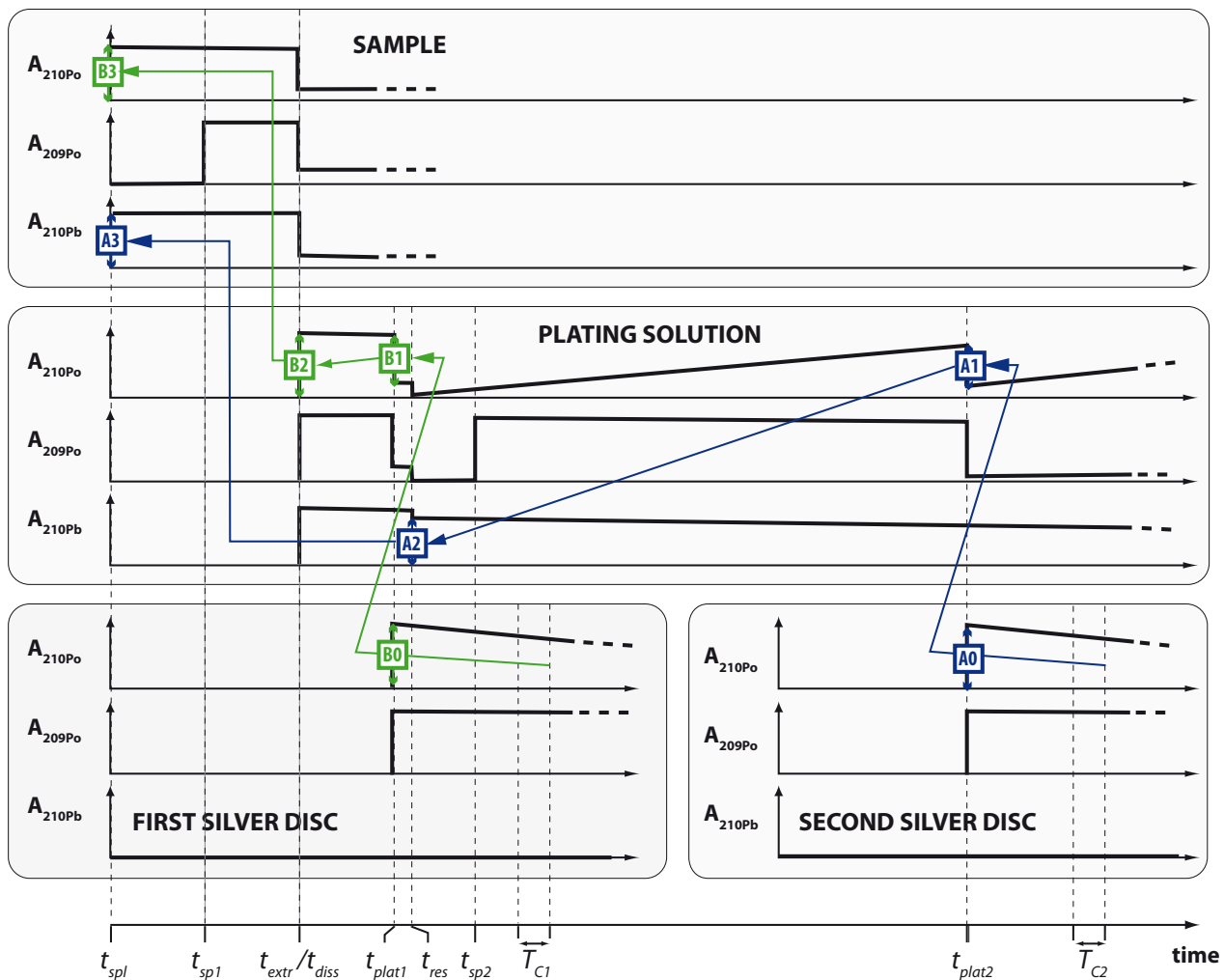


Figure 2: Schematic representation showing the temporal evolution of the activities of ^{210}Po , ^{209}Po and ^{210}Pb in the sample (total, dissolved or particulate), plating solution and silver discs during sample processing (from the left to the right). The steps followed to calculate the initial activity of ^{210}Pb (steps A) and ^{210}Po (steps B) in the sample are indicated.

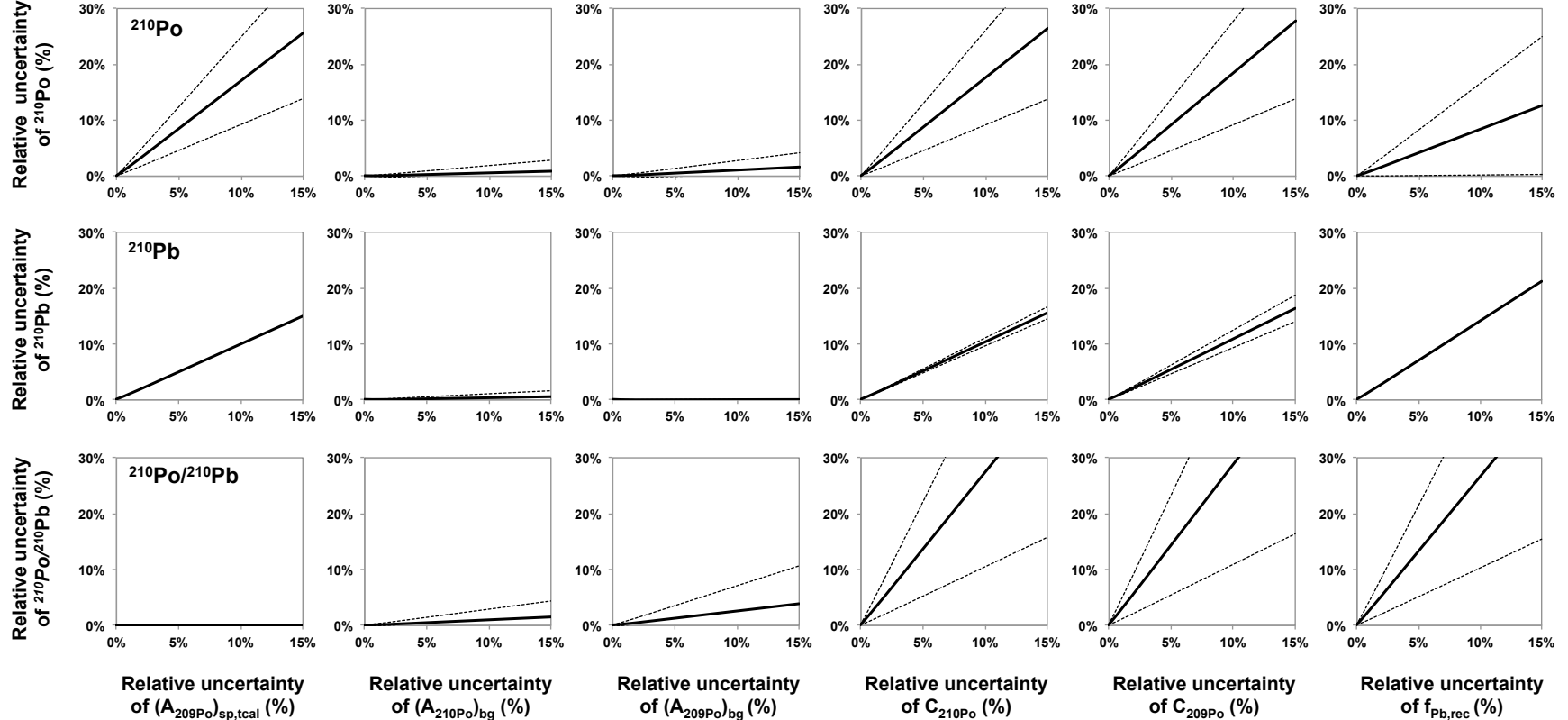


Figure 3: Evolution of the total relative uncertainty on the calculated ^{210}Po and ^{210}Pb activities and $^{210}\text{Po}/^{210}\text{Pb}$ activity ratios as a function of the relative uncertainty on parameters considered for the calculations of the activities of ^{210}Po and ^{210}Pb . The full line corresponds to the mean, and the dashed lines to the ± 1 standard deviation around the mean. They were calculated using the experimental data from the processing of 200 seawater samples by varying their individual relative uncertainty from 0 to 15%, while keeping the relative uncertainty on other parameters to 0%.

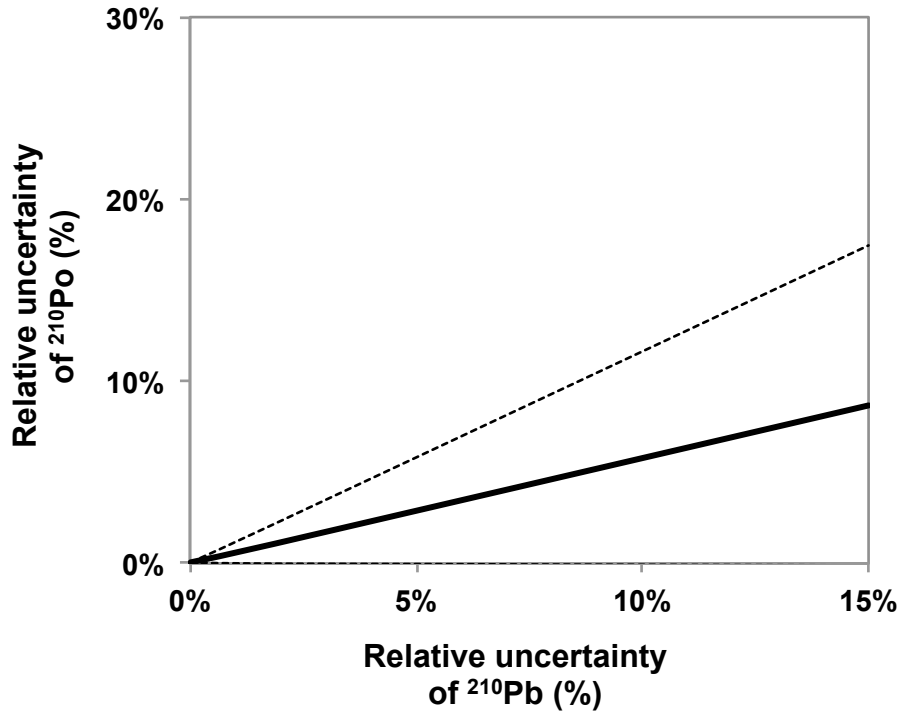


Figure 4: Evolution of the final relative uncertainty of ^{210}Po as a function of the final relative uncertainty of the ^{210}Pb activity. The full line corresponds to the mean, and the dashed lines to the ± 1 standard deviation around the mean (note that the lower dashed line can not be distinguished from the X-axis). They were calculated using the experimental data from the processing of 200 seawater samples by varying the relative uncertainty of ^{210}Pb from 0 to 15%, while keeping the relative uncertainty of all other parameters at 0%.

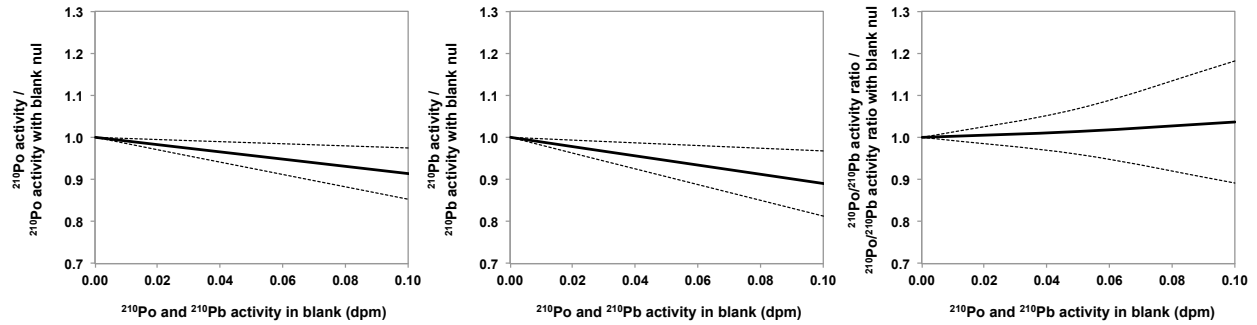


Figure 5: Influence of ^{210}Po and ^{210}Pb activities within blanks on ^{210}Po and ^{210}Pb activities and $^{210}\text{Po}/^{210}\text{Pb}$ activity ratios (expressed as the ratio between calculated values for the range of blank activity tested and the activity calculated with a null blank). The full line corresponds to the mean, and the dashed lines to the ± 1 standard deviation around the mean. They were calculated using the experimental data from the processing of 200 seawater samples.

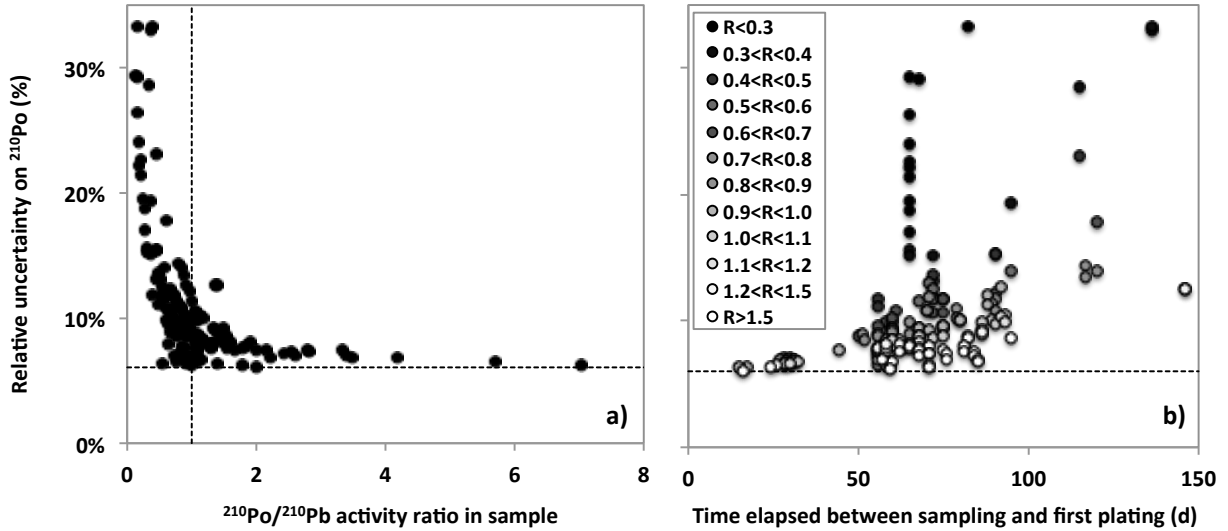


Figure 6: Relative uncertainty on the final calculated ^{210}Po activity as a function of a) $^{210}\text{Po}/^{210}\text{Pb}$ activity ratio in the sample at sampling time and b) time elapsed between sampling and first plating. These were estimated assuming relative uncertainties of 3% for the ^{209}Po spike calibration, 3.5% for the counting statistics and 3% for the Pb recovery, for the 200 samples representing typical experimental and environmental conditions presented in the text. The Y-axis is the same for both panels. The vertical dashed line represents the $^{210}\text{Po}/^{210}\text{Pb}$ activity ratio of 1. The horizontal dashed line represents the lowest ^{210}Po relative uncertainty obtained under these conditions, 6%. R corresponds to the $^{210}\text{Po}/^{210}\text{Pb}$ activity ratio. In b), the data with high (>13%) relative uncertainty on ^{210}Po and plated 65-70 days after collection, correspond to samples with quite low $^{210}\text{Po}/^{210}\text{Pb}$ activity ratios (<0.3) and were mostly dissolved surface samples from different stations, that were by chance processed with similar time delays.

Tables

Table 1: List of parameters used in the calculations with their dimension and definition

Parameter	Dimension	Definition
CONSTANTS		
λ_{210Pb}	min ⁻¹	²¹⁰ Pb decay constant
λ_{209Po}	min ⁻¹	²⁰⁹ Po decay constant
λ_{210Po}	min ⁻¹	²¹⁰ Po decay constant
SAMPLE INFORMATION		
t_{spl}		Sampling date
m_{spl}	kg	Mass of the sample.
DETECTOR INFORMATION		
ε		Detector efficiency
$(A_{210Po})_{bg,1}$ and $(A_{210Po})_{bg,2}$	cpm	First and second detector background for ²¹⁰ Po
$(A_{209Po})_{bg,1}$ and $(A_{209Po})_{bg,2}$	cpm	First and second detector background for ²⁰⁹ Po
PROCESSING & ANALYSIS INFORMATION		
t_{sp1} and t_{sp2}		First and second spike addition dates
t_{extr} and t_{diss}		Extraction (filtered or unfiltered samples) or dissolution (particulate samples) dates
t_{plat1} and t_{plat2}		First and second plating dates
$t_{c1,st}$ and $t_{c2,st}$		Starting dates of the first and second counting
T_{C1} or T_{C2}	min	First and second counting times
t_{res}		Resin separation date
t_{car}		Carrier addition date
$t_{sp,cal}$		²⁰⁹ Po spike calibration date
m_{sp1} and m_{sp2}	g	First and second masses of the ²⁰⁹ Po spikes added
$C_{210Po,1}$ and $C_{210Po,2}$	cp	Total counts of ²¹⁰ Po during the first and second counting
$C_{209Po,1}$ and $C_{209Po,2}$	cp	Total counts of ²⁰⁹ Po during the first and second counting
$(A_{209Po})_{sp,t_{cal}}$	dpm.g ⁻¹	²⁰⁹ Po activity in the spike at the date of calibration
m_{a11}	g	Mass of the first aliquot of the plating solution collected after the first plating for stable Pb analysis.
m_c	g	Mass of Pb carrier solution added in the sample.
m_{sol1} and m_{sol2}	g	Mass of the plating solution when the first and second aliquots for stable Pb analysis were collected
$[Pb]_c$, $[Pb]_{sol1}$ and $[Pb]_{sol2}$	μg.g ⁻¹	Pb concentration in the carrier solution and in the plating solution when the first and second aliquots for stable Pb analysis were collected
CALCULATED PARAMETERS		
$f_{Po,rec1}$ and $f_{Po,rec2}$		First and second Po recovery efficiencies
$f_{Pb,rec1}$ and $f_{Pb,rec_{tot}}$		Pb recovery efficiencies during extraction/dissolution only and during total sample processing (including also resin separation step) respectively
$(A_{210Po})_B$ and $(A_{210Pb})_B$	dpm	²¹⁰ Po and ²¹⁰ Pb activity in the blank, corresponding to their respective activity brought with carrier addition
$(A_{210Po})_{sol,t_{plat1}}$ and $(A_{210Po})_{sol,t_{plat2}}$	dpm	²¹⁰ Po activity in the plating solution at the first and second plating dates respectively
$(A_{210Pb})_{sol,t_{res}}$	dpm	²¹⁰ Pb activity in the plating solution at the resin separation date
$(A_{210Po})_{sol,t_{extr}}$ and $(A_{210Po})_{sol,t_{diss}}$	dpm	²¹⁰ Po activity in the plating solution at the extraction (filtered or unfiltered samples) or dissolution (particulate samples) dates
$(A_{210Pb})_{spl,t_{spl}}$ and $(A_{210Po})_{spl,t_{spl}}$	dpm	²¹⁰ Pb and ²¹⁰ Po activity in the sample at the sampling date
$(A_{210Pb})_{spl,t_{spl}} \left(\frac{dpm}{100kg}\right)$ and $(A_{210Po})_{spl,t_{spl}} \left(\frac{dpm}{100kg}\right)$	dpm.100kg ⁻¹	²¹⁰ Pb and ²¹⁰ Po activity in the sample at the sampling date

Table 2: Range of values for the parameters considered for typical experimental and environmental conditions. These originate from about 200 data representing dissolved, particulate or total seawater samples processed for ^{210}Po and ^{210}Pb determination.

Considered parameters in the uncertainty calculation*	Range of reported values (n=189)
$(A_{209\text{Po}})_{\text{sp, total}}$ (dpm/g)	1.3-53.4
$(A_{210\text{Po}})_{\text{bg}}$ (dpm)	<0.001-0.014
$(A_{209\text{Po}})_{\text{bg}}$ (dpm)	<0.001-0.047
$C_{210\text{Po}}$ (counts)	100-2700
$C_{209\text{Po}}$ (counts)	130-6700
$f_{\text{Pb, rec}}$ (%)	15-112

*parameters from the steps A and B of samples processing are here combined

A methods assessment and recommendations for improving calculations and reducing uncertainties in the determination of ^{210}Po and ^{210}Pb activities in seawater

S. Rigaud¹, V. Puigcorb ^{2,3}, P. C mara-Mor^{2,3}, N. Casacuberta^{2,3}, M. Roca-Mart ^{2,3}, J. Garcia-Orellana^{2,3}, C. R. Benitez-Nelson⁴, P. Masqu ^{2,3}, and T. Church¹

¹School of Marine Science and Policy, University of Delaware, Newark, Delaware 19716 USA.

²Departament de F sica, Universitat Aut noma de Barcelona, Barcelona 08193 Spain.

³Institut de Ci ncia i Tecnologia Ambientals, Universitat Aut noma de Barcelona, Barcelona 08193 Spain.

⁴Marine Science Program and Department of Earth and Ocean Sciences, University of South Carolina, South Carolina 29208 USA.

Equations Appendix A

Eq. 1a

$$(A_{210\text{Po}})_{\text{sol},t_{\text{plat}2}} = \left(\frac{C_{210\text{Po},2}}{T_{c2}} - (A_{210\text{Po}})_{\text{bg},2} \right) \frac{\lambda_{210\text{Po}} T_{c2}}{1 - e^{-\lambda_{210\text{Po}} T_{c2}}} \frac{(A_{209\text{Po}})_{\text{sp},t_{\text{cal}}} e^{-\lambda_{209\text{Po}}(t_{c2,\text{st}} - t_{\text{sp},\text{cal}})} m_{\text{sp}2}}{\left(\frac{C_{209\text{Po},2}}{T_{c2}} - (A_{209\text{Po}})_{\text{bg},2} \right) \frac{\lambda_{209\text{Po}} T_{c2}}{1 - e^{-\lambda_{209\text{Po}} T_{c2}}}} e^{\lambda_{210\text{Po}}(t_{c2,\text{st}} - t_{\text{plat}2})}$$

Eq. 1b

$$\begin{aligned}
 \sigma((A_{210Po})_{sol,t_{plat2}}) = & \sqrt{ \sigma(C_{210Po,2})^2 \left(\frac{\lambda_{210Po}}{1 - e^{-\lambda_{210Po}T_{c2}}} \frac{(A_{209Po})_{sp,t_{cal}} e^{-\lambda_{209Po}(t_{c2,st} - t_{sp,cal})} m_{sp2}}{\left(\frac{C_{209Po,2}}{T_{c2}} - (A_{209Po})_{bg,2} \right) \frac{\lambda_{209Po}T_{c2}}{1 - e^{-\lambda_{209Po}T_{c2}}}} e^{\lambda_{210Po}(t_{c2,st} - t_{plat2})} \right)^2 } \\
 & + \sigma((A_{210Po})_{bg,2})^2 \left(\frac{\lambda_{210Po}T_{c2}}{1 - e^{-\lambda_{210Po}T_{c2}}} \frac{(A_{209Po})_{sp,t_{cal}} e^{-\lambda_{209Po}(t_{c2,st} - t_{sp,cal})} m_{sp2}}{\left(\frac{C_{209Po,2}}{T_{c2}} - (A_{209Po})_{bg,2} \right) \frac{\lambda_{209Po}T_{c2}}{1 - e^{-\lambda_{209Po}T_{c2}}}} e^{\lambda_{210Po}(t_{c2,st} - t_{plat2})} \right)^2 \\
 & + \sigma((A_{209Po})_{sp,t_{cal}})^2 \left(\left(\frac{C_{210Po,2}}{T_{c2}} - (A_{210Po})_{bg,2} \right) \frac{\lambda_{210Po}T_{c2}}{1 - e^{-\lambda_{210Po}T_{c2}}} \frac{e^{-\lambda_{209Po}(t_{c2,st} - t_{sp,cal})} m_{sp2}}{\left(\frac{C_{209Po,2}}{T_{c2}} - (A_{209Po})_{bg,2} \right) \frac{\lambda_{209Po}T_{c2}}{1 - e^{-\lambda_{209Po}T_{c2}}}} e^{\lambda_{210Po}(t_{c2,st} - t_{plat2})} \right)^2 \\
 & + \sigma(C_{209Po,2})^2 \left(\left(\frac{C_{210Po,2}}{T_{c2}} - (A_{210Po})_{bg,2} \right) \frac{\lambda_{210Po}T_{c2}}{1 - e^{-\lambda_{210Po}T_{c2}}} \frac{(A_{209Po})_{sp,t_{cal}} e^{-\lambda_{209Po}(t_{c2,st} - t_{sp,cal})} m_{sp2}}{\left(C_{209Po,2} - T_{c2}(A_{209Po})_{bg,2} \right)^2 \frac{\lambda_{209Po}}{1 - e^{-\lambda_{209Po}T_{c2}}}} e^{\lambda_{210Po}(t_{c2,st} - t_{plat2})} \right)^2 \\
 & + \sigma((A_{209Po})_{bg,2})^2 \left(\left(\frac{C_{210Po,2}}{T_{c2}} - (A_{210Po})_{bg,2} \right) \frac{\lambda_{210Po}T_{c2}}{1 - e^{-\lambda_{210Po}T_{c2}}} \frac{(A_{209Po})_{sp,t_{cal}} e^{-\lambda_{209Po}(t_{c2,st} - t_{sp,cal})} m_{sp2} T_{c2}}{\left(C_{209Po,2} - T_{c2}(A_{209Po})_{bg,2} \right)^2 \frac{\lambda_{209Po}}{1 - e^{-\lambda_{209Po}T_{c2}}}} e^{\lambda_{210Po}(t_{c2,st} - t_{plat2})} \right)^2
 \end{aligned}$$

Eq. 2a

$$f_{Po_{rec2}} = \frac{\left(\frac{C_{209Po,2}}{T_{c2}} - (A_{209Po})_{bg} \right) \frac{\lambda_{209Po}T_{c2}}{1 - e^{-\lambda_{209Po}T_{c2}}}}{\varepsilon(A_{209Po})_{sp,t_{cal}} e^{-\lambda_{209Po}(t_{c2,st} - t_{sp,cal})} m_{sp2}}$$

Eq. 3a

$$(A_{210Pb})_{sol,t_{res}} = \frac{(A_{210Po})_{sol,t_{plat2}} (\lambda_{210Po} - \lambda_{210Pb})}{\lambda_{210Po} (e^{-\lambda_{210Pb}(t_{plat2}-t_{res})} - e^{-\lambda_{210Po}(t_{plat2}-t_{res})})}$$

Eq. 3b

$$\sigma((A_{210Pb})_{sol,t_{res}}) = \sqrt{\sigma((A_{210Po})_{sol,t_{plat2}})^2 \left(\frac{(\lambda_{210Po} - \lambda_{210Pb})}{\lambda_{210Po} (e^{-\lambda_{210Pb}(t_{plat2}-t_{res})} - e^{-\lambda_{210Po}(t_{plat2}-t_{res})})} \right)^2}$$

Eq. 4a

$$(A_{210Pb})_{spl,t_{spl}} = \frac{(A_{210Pb})_{sol,t_{res}} e^{\lambda_{210Pb}(t_{res}-t_{spl})}}{f_{Pb_{rec,tot}}} \left(1 + \frac{m_{al1}}{m_{sol1}} \right) - (A_{210Pb})_B$$

Eq. 4b

$$\sigma((A_{210Pb})_{spl,t_{spl}}) = \sqrt{\sigma((A_{210Pb})_{sol,t_{res}})^2 \left(\frac{e^{\lambda_{210Pb}(t_{res}-t_{spl})}}{f_{Pb_{rec,tot}}} \left(1 + \frac{m_{al1}}{m_{sol1}} \right) \right)^2 + \sigma(f_{Pb_{rec,tot}})^2 \left(\frac{(A_{210Pb})_{sol,t_{res}} e^{\lambda_{210Pb}(t_{res}-t_{spl})}}{(f_{Pb_{rec,tot}})^2} \left(1 + \frac{m_{al1}}{m_{sol1}} \right) \right)^2 + \sigma((A_{210Pb})_B)^2}$$

Eq. 5a

$$f_{Pb_{rec,tot}} = \frac{m_{sol2}[Pb]_{sol2} + m_{al1}[Pb]_{sol1}}{m_c[Pb]_c}$$

Eq. 5b

$$\sigma(f_{Pb_{rec,tot}}) = \sqrt{\begin{aligned} &\sigma([Pb]_{sol2})^2 \left(\frac{m_{sol2}}{m_c[Pb]_c}\right)^2 \\ &+ \sigma([Pb]_{sol1})^2 \left(\frac{m_{al1}}{m_c[Pb]_c}\right)^2 \\ &+ \sigma([Pb]_c)^2 \left(\frac{m_{sol2}[Pb]_{sol2} + m_{al1}[Pb]_{sol1}}{m_c[Pb]_c}\right)^2 \end{aligned}}$$

Eq. 6a

$$(A_{210Pb})_B = \frac{(A_{210Pb})_{sol,t_{res}} e^{\lambda_{210Pb}(t_{res}-t_{car})}}{f_{Pb_{rec,tot}}} \left(1 + \frac{m_{al1}}{m_{sol1}}\right)$$

Eq. 6b

$$\sigma((A_{210Pb})_B) = \sqrt{\begin{aligned} &\sigma((A_{210Pb})_{sol,t_{res}})^2 \left(\frac{e^{\lambda_{210Pb}(t_{res}-t_{car})}}{f_{Pb_{rec,tot}}} \left(1 + \frac{m_{al1}}{m_{sol1}}\right)\right)^2 \\ &+ \sigma(f_{Pb_{rec,tot}})^2 \left(\frac{(A_{210Pb})_{sol,t_{res}} e^{\lambda_{210Pb}(t_{res}-t_{car})}}{(f_{Pb_{rec,tot}})^2} \left(1 + \frac{m_{al1}}{m_{sol1}}\right)\right)^2 \end{aligned}}$$

Eq. 7a

$$(A_{210Pb})_{spl,t_{spl}} \left(\frac{dpm}{100kg} \right) = \frac{(A_{210Pb})_{spl,t_{spl}}}{m_{spl}} 100$$

Eq. 7b

$$\sigma \left((A_{210Pb})_{spl,t_{spl}} \left(\frac{dpm}{100kg} \right) \right) = \sqrt{\sigma \left((A_{210Pb})_{spl,t_{spl}} \right)^2 \left(\frac{100}{m_{spl}} \right)^2}$$

Eq. 8a

$$(A_{210Po})_{sol,t_{plat1}} = \left(\frac{C_{210Po,1}}{T_{c1}} - (A_{210Po})_{bg,1} \right) \frac{\lambda_{210Po} T_{c1}}{1 - e^{-\lambda_{210Po} T_{c1}}} \frac{(A_{209Po})_{sp,t_{cal}} e^{-\lambda_{209Po}(t_{c1,st} - t_{sp,cal})} m_{sp1}}{\left(\frac{C_{209Po,1}}{T_{c1}} - (A_{209Po})_{bg,1} \right) \frac{\lambda_{209Po} T_{c1}}{1 - e^{-\lambda_{209Po} T_{c1}}}} e^{\lambda_{210Po}(t_{c1,st} - t_{plat1})}$$

Eq. 8b

$$\sigma((A_{210Po})_{sol,t_{plat1}}) = \sqrt{\begin{aligned} & \sigma(C_{210Po,1})^2 \left(\frac{\lambda_{210Po}}{1 - e^{-\lambda_{210Po}T_{c1}}} \frac{(A_{209Po})_{sp,t_{cal}} e^{-\lambda_{209Po}(t_{c1,st}-t_{sp,cal})} m_{sp1}}{\left(\frac{C_{209Po,1}}{T_{c1}} - (A_{209Po})_{bg,1}\right) \frac{\lambda_{209Po}T_{c1}}{1 - e^{-\lambda_{209Po}T_{c1}}}} e^{\lambda_{210Po}(t_{c1,st}-t_{plat1})} \right)^2 \\ & + \sigma((A_{210Po})_{bg,1})^2 \left(\frac{\lambda_{210Po}T_{c1}}{1 - e^{-\lambda_{210Po}T_{c1}}} \frac{(A_{209Po})_{sp,t_{cal}} e^{-\lambda_{209Po}(t_{c1,st}-t_{sp,cal})} m_{sp1}}{\left(\frac{C_{209Po,1}}{T_{c1}} - (A_{209Po})_{bg,1}\right) \frac{\lambda_{209Po}T_{c1}}{1 - e^{-\lambda_{209Po}T_{c1}}}} e^{\lambda_{210Po}(t_{c1,st}-t_{plat1})} \right)^2 \\ & + \sigma((A_{209Po})_{sp,t_{cal}})^2 \left(\left(\frac{C_{210Po,1}}{T_{c1}} - (A_{210Po})_{bg,1}\right) \frac{\lambda_{210Po}T_{c1}}{1 - e^{-\lambda_{210Po}T_{c1}}} \frac{e^{-\lambda_{209Po}(t_{c1,st}-t_{sp,cal})} m_{sp1}}{\left(\frac{C_{209Po,1}}{T_{c1}} - (A_{209Po})_{bg,1}\right) \frac{\lambda_{209Po}T_{c1}}{1 - e^{-\lambda_{209Po}T_{c1}}}} e^{\lambda_{210Po}(t_{c1,st}-t_{plat1})} \right)^2 \\ & + \sigma(C_{209Po,1})^2 \left(\left(\frac{C_{210Po,1}}{T_{c1}} - (A_{210Po})_{bg,1}\right) \frac{\lambda_{210Po}T_{c1}}{1 - e^{-\lambda_{210Po}T_{c1}}} \frac{(A_{209Po})_{sp,t_{cal}} e^{-\lambda_{209Po}(t_{c1,st}-t_{sp,cal})} m_{sp1}}{(C_{209Po,1} - T_{c1})(A_{209Po})_{bg,1}} \frac{\lambda_{209Po}}{1 - e^{-\lambda_{209Po}T_{c1}}} e^{\lambda_{210Po}(t_{c1,st}-t_{plat1})} \right)^2 \\ & + \sigma((A_{209Po})_{bg,1})^2 \left(\left(\frac{C_{210Po,1}}{T_{c1}} - (A_{210Po})_{bg,1}\right) \frac{\lambda_{210Po}T_{c1}}{1 - e^{-\lambda_{210Po}T_{c1}}} \frac{(A_{209Po})_{sp,t_{cal}} e^{-\lambda_{209Po}(t_{c1,st}-t_{sp,cal})} m_{sp1}T_{c1}}{(C_{209Po,1} - T_{c1})(A_{209Po})_{bg,1}} \frac{\lambda_{209Po}}{1 - e^{-\lambda_{209Po}T_{c1}}} e^{\lambda_{210Po}(t_{c1,st}-t_{plat1})} \right)^2 \end{aligned}}$$

Eq. 9a

$$(A_{210Po})_{sol,t_{extr}} = \left((A_{210Po})_{sol,t_{plat1}} - \frac{\lambda_{210Po} \left((A_{210Pb})_{spl,t_{spl}} e^{-\lambda_{210Pb}(t_{extr}-t_{spl})} + (A_{210Pb})_B e^{-\lambda_{210Pb}(t_{extr}-t_{car})} \right) f_{Pb_{rec1}} \left(e^{-\lambda_{210Pb}(t_{plat1}-t_{extr})} - e^{-\lambda_{210Po}(t_{plat1}-t_{extr})} \right)}{\lambda_{210Po} - \lambda_{210Pb}} \right) e^{\lambda_{210Po}(t_{plat1}-t_{extr})}$$

Eq. 9b

$$\sigma((A_{210Po})_{sol,t_{extr}}) = \sqrt{\begin{aligned} & \sigma((A_{210Po})_{sol,t_{plat1}})^2 (e^{\lambda_{210Po}(t_{plat1}-t_{extr})})^2 \\ & + \sigma((A_{210Pb})_{spl,t_{spl}})^2 \left(\frac{\lambda_{210Po} e^{-\lambda_{210Pb}(t_{extr}-t_{spl})} f_{Pb_{rec1}}}{\lambda_{210Po} - \lambda_{210Pb}} (e^{-\lambda_{210Pb}(t_{plat1}-t_{extr})} - e^{-\lambda_{210Po}(t_{plat1}-t_{extr})}) e^{\lambda_{210Po}(t_{plat1}-t_{extr})} \right)^2 \\ & + \sigma((A_{210Pb})_B)^2 \left(\frac{\lambda_{210Po} e^{-\lambda_{210Pb}(t_{extr}-t_{car})} f_{Pb_{rec1}}}{\lambda_{210Po} - \lambda_{210Pb}} (e^{-\lambda_{210Pb}(t_{plat1}-t_{extr})} - e^{-\lambda_{210Po}(t_{plat1}-t_{extr})}) e^{\lambda_{210Po}(t_{plat1}-t_{extr})} \right)^2 \\ & + \sigma(f_{Pb_{rec1}})^2 \left(\frac{\lambda_{210Po} \left((A_{210Pb})_{spl,t_{spl}} e^{-\lambda_{210Pb}(t_{extr}-t_{spl})} + (A_{210Pb})_B e^{-\lambda_{210Pb}(t_{extr}-t_{car})} \right)}{(\lambda_{210Po} - \lambda_{210Pb}) (e^{-\lambda_{210Pb}(t_{plat1}-t_{extr})} - e^{-\lambda_{210Po}(t_{plat1}-t_{extr})}) e^{\lambda_{210Po}(t_{plat1}-t_{extr})}} \right)^2 \end{aligned}}$$

Eq. 10a

$$f_{Pb_{rec1}} = \frac{m_{sol1}[Pb]_{sol1}}{m_c[Pb]_c}$$

Eq. 10b

$$\sigma(f_{Pb_{rec1}}) = \sqrt{\sigma([Pb]_{sol1})^2 \left(\frac{m_{sol1}}{m_c[Pb]_c} \right)^2 + \sigma([Pb]_c)^2 \left(\frac{m_{sol1}[Pb]_{sol1}}{m_c[Pb]_c^2} \right)^2}$$

Eq. 11a

$$(A_{210Po})_{spl,t_{spl}} = (A_{210Po})_{sol,t_{extr}} e^{\lambda_{210Po}(t_{extr}-t_{spl})} - \frac{\lambda_{210Po}(A_{210Pb})_{spl,t_{spl}}}{\lambda_{210Po} - \lambda_{210Pb}} \left(e^{-\lambda_{210Pb}(t_{extr}-t_{spl})} - e^{-\lambda_{210Po}(t_{extr}-t_{spl})} \right) e^{\lambda_{210Po}(t_{extr}-t_{spl})}$$

$$- \frac{\lambda_{210Po}(A_{210Pb})_B}{\lambda_{210Po} - \lambda_{210Pb}} \left(e^{-\lambda_{210Pb}(t_{extr}-t_{car})} - e^{-\lambda_{210Po}(t_{extr}-t_{car})} \right) e^{\lambda_{210Po}(t_{extr}-t_{car})} - (A_{210Po})_B$$

Eq. 11b

$$\sigma \left((A_{210Po})_{spl,t_{spl}} \right) = \sqrt{\begin{aligned} & \sigma \left((A_{210Po})_{sol,t_{extr}} \right)^2 \left(e^{\lambda_{210Po}(t_{extr}-t_{spl})} \right)^2 \\ & + \sigma \left((A_{210Pb})_{spl,t_{spl}} \right)^2 \left(\frac{\lambda_{210Po}}{\lambda_{210Po} - \lambda_{210Pb}} \left(e^{-\lambda_{210Pb}(t_{extr}-t_{spl})} - e^{-\lambda_{210Po}(t_{extr}-t_{spl})} \right) e^{\lambda_{210Po}(t_{extr}-t_{spl})} \right)^2 \\ & + \sigma \left((A_{210Pb})_B \right)^2 \left(\frac{\lambda_{210Po}}{\lambda_{210Po} - \lambda_{210Pb}} \left(e^{-\lambda_{210Pb}(t_{extr}-t_{car})} - e^{-\lambda_{210Po}(t_{extr}-t_{car})} \right) e^{\lambda_{210Po}(t_{extr}-t_{car})} \right)^2 \\ & + \sigma \left((A_{210Po})_B \right)^2 \end{aligned}}$$

Eq. 12a

$$(A_{210Po})_B = (A_{210Po})_{sol,t_{plat1}} e^{\lambda_{210Po}(t_{plat1}-t_{car})} - \frac{\lambda_{210Po}(A_{210Pb})_B e^{-\lambda_{210Pb}(t_{extr}-t_{car})} f_{Pb_{rec1}}}{\lambda_{210Po} - \lambda_{210Pb}} \left(e^{-\lambda_{210Pb}(t_{plat1}-t_{extr})} - e^{-\lambda_{210Po}(t_{plat1}-t_{extr})} \right) e^{\lambda_{210Po}(t_{plat1}-t_{extr})}$$

$$- \frac{\lambda_{210Po}(A_{210Pb})_B}{\lambda_{210Po} - \lambda_{210Pb}} \left(e^{-\lambda_{210Pb}(t_{extr}-t_{car})} - e^{-\lambda_{210Po}(t_{extr}-t_{car})} \right) e^{\lambda_{210Po}(t_{extr}-t_{car})}$$

Eq. 12b

$$\sigma((A_{210Po})_B) = \sqrt{\begin{aligned} & \sigma((A_{210Po})_{sol,t_{plat1}})^2 \left(e^{\lambda_{210Po}(t_{plat1}-t_{car})} \right)^2 \\ & + \sigma((A_{210Pb})_B)^2 \left(\frac{\lambda_{210Po} e^{-\lambda_{210Pb}(t_{extr}-t_{car})} f_{Pbrec1}}{\lambda_{210Po} - \lambda_{210Pb}} \left(e^{-\lambda_{210Pb}(t_{plat1}-t_{extr})} - e^{-\lambda_{210Po}(t_{plat1}-t_{extr})} \right) e^{\lambda_{210Po}(t_{plat1}-t_{extr})} \right)^2 \\ & + \sigma((A_{210Pb})_B)^2 \left(\frac{\lambda_{210Po}}{\lambda_{210Po} - \lambda_{210Pb}} \left(e^{-\lambda_{210Pb}(t_{extr}-t_{car})} - e^{-\lambda_{210Po}(t_{extr}-t_{car})} \right) e^{\lambda_{210Po}(t_{extr}-t_{car})} \right)^2 \\ & + \sigma(f_{Pbrec1})^2 \left(\frac{\lambda_{210Po} (A_{210Pb})_B e^{-\lambda_{210Pb}(t_{extr}-t_{car})}}{\lambda_{210Po} - \lambda_{210Pb}} \left(e^{-\lambda_{210Pb}(t_{plat1}-t_{extr})} - e^{-\lambda_{210Po}(t_{plat1}-t_{extr})} \right) e^{\lambda_{210Po}(t_{plat1}-t_{extr})} \right)^2 \end{aligned}}$$

Eq. 13a

$$(A_{210Po})_{spl,t_{spl}} \left(\frac{dpm}{100kg} \right) = \frac{(A_{210Po})_{spl,t_{spl}}}{m_{spl}} 100$$

Eq. 13b

$$\sigma \left((A_{210Po})_{spl,t_{spl}} \left(\frac{dpm}{100kg} \right) \right) = \sqrt{\sigma \left((A_{210Po})_{spl,t_{spl}} \right)^2 \left(\frac{100}{m_{spl}} \right)^2}$$

